

EFFECT OF INELASTIC BEHAVIOUR OF LOAD BEARING WALLS ON
THE FRAME–WALL STRUCTURAL SYSTEMS

A THESIS SUBMITTED TO
THE GRADUATE SCHOOL OF NATURAL AND APPLIED SCIENCES
OF
MIDDLE EAST TECHNICAL UNIVERSITY

BY

GÖKAY GÜLER

IN PARTIAL FULFILLMENT OF THE REQUIREMENTS
FOR
THE DEGREE OF MASTER OF SCIENCE
IN
CIVIL ENGINEERING

MAY 2009

Approval of the thesis:

**EFFECT OF INELASTIC BEHAVIOUR OF LOAD BEARING WALLS
ON THE FRAME-WALL STRUCTURAL SYSTEMS**

Submitted by **GÖKAY GÜLER** in partial fulfillment of the requirements for
the degree of **Master of Science in Civil Engineering Department,**
Middle East Technical University by,

Prof. Dr. Canan Özgen

Dean, Graduate School of **Natural and Applied Sciences**

Prof. Dr. Güney Özcebe

Head of Department, **Civil Engineering**

Inst. Dr. Afşin Sarıtaş

Supervisor, **Civil Engineering Dept., METU**

Examining Committee Members

Prof. Dr. Mehmet Utku

Civil Engineering, METU

Inst. Dr. Afşin Sarıtaş

Civil Engineering, METU

Assoc. Prof. Dr. Barış Binici

Civil Engineering, METU

Asst. Prof. Dr. Alp Caner

Civil Engineering, METU

Asst. Prof. Dr. Eray Baran

Civil Engineering, Atılım University

Date: 22.05.2009

I hereby declare that all information in this document has been obtained and presented in accordance with academic rules and ethical conduct. I also declare that, as required by these rules and conduct, I have fully cited and referenced all material and results that are not original to this work.

Name, Lastname : Gökay Güler

Signature :

ABSTRACT

EFFECT OF INELASTIC BEHAVIOUR OF LOAD BEARING WALLS ON THE FRAME-WALL STRUCTURAL SYSTEMS

GÜLER, Gökay

**M.S., Department of Civil Engineering
Supervisor: Inst. Dr. Afşin Sarıtaş**

May 2009, 72 pages

The purpose of this study is to investigate the influence of material and geometric nonlinearities occurring in beams, columns and walls of RC frame-wall structural systems when undergoing severe ground excitations. For this purpose, a low-rise RC building is considered with and without walls, and the joining beams and columns are designed with the strong-column weak-beam concept. The dimensions, material properties and the reinforcement amounts are calculated in accordance with the values suggested in design codes. Each structure is analyzed for various levels of applied vertical force and change in wall stiffness; where the effect of geometric nonlinearity is considered for each case. Force formulation frame elements with spreading inelasticity over the span are used for the modelling of each beam, column and wall. The coupling of the section forces is obtained by the fibre discretization of the section into several material points. Each section is divided into confined and

unconfined regions and appropriate material properties are used for concrete and steel for cyclic loading. Both static pushover and dynamic analyses are performed in order to replicate the worst case scenario for a possible earthquake. From this study, it is concluded that the beams and columns of a frame-wall structural system should be designed carefully for load redistributions resulting from the yielding of the wall in the case of a strong earthquake, thus the design codes should address this situation for both in the retrofit of existing frame buildings with walls and in the construction of new frame-wall type buildings.

Keywords: Frame-wall system, structural wall, inelastic response.

ÖZ

BETONARME TAŞIYICI DUVARLARIN ELASTİK OLMAYAN DAVRANIŞLARININ ÇERÇEVE-DUVAR SİSTEMLERİ ÜZERİNDEKİ ETKİLERİ

GÜLER, Gökay

Yüksek Lisans, İnşaat Mühendisliği Bölümü

Tez Yöneticisi: Öğr. Gör. Dr. Afşin Sarıtaş

Mayıs 2009, 72 sayfa

Bu çalışmanın amacı kiriş, kolon ve betonarme çerçeve-duvar sistemlerinin yer sarsıntıları sırasında, doğrusal olmayan malzeme ve geometri özelliklerine duyarlılığını araştırmaktır. Bu amaca uygun olarak, alçak katlı duvarlı ve duvarsız yapısal sistemler seçilmiş ve kiriş-kolon düzenekleri güçlü-kolon zayıf-kiriş dizayn yöntemine göre tasarlanmıştır. Yapının boyutları, malzeme özellikleri ve donatı miktarları yönetmeliğe uygun olarak seçilmiştir. Bütün yapılar artan düşey yükler ve değişken duvar duyarlılığına (rijitlik) göre çözümlenmiş ve her çözümlemede doğrusal olmayan geometri göz önüne alınmıştır. Kolon, kiriş ve duvar modellemesinde inelastik malzeme özelliğini eleman boyunca yayan ve karma formulasyonla modellenmiş çerçeve elemanları kullanılmıştır.

Kesit üstündeki malzeme noktalarının entegrasyonu sonucu kesit kuvvetleri arasındaki bağlantı kurulmuş, yani fiber kesit modeli kullanılmıştır. Her bir kesit, sargılı ve sargısız bölgeler olarak ayrılmış ve beton ve çelik için gerçekçi periyodik malzeme modelleri kullanılmıştır. Olası bir deprem için en kötü senaryo durumunu göstermek için hem statik öteleme hem de dinamik analiz gerçekleştirilmiştir. Bu çalışma sonunda, çerçeve-duvar sistemleri tasarımında güçlü bir deprem sırasında duvarda oluşan doğrusal olmayan davranış sonucu ortaya çıkan yük dağılımının dikkate alınması gerektiği anlaşılmaktadır. Dolayısıyla yönetmelikte, çerçeve binaların duvarla güçlendirilmesi veya yeni yapılacak çerçeve-duvar sistemlerinin dizayn ve analizinde bu konu dikkate alınmalıdır.

Anahtar Kelimeler: Çerçeve–duvar sistemi, taşıyıcı duvar, doğrusal olmayan davranış.

To my family...

ACKNOWLEDGEMENTS

This study was accomplished under the supervision of Inst. Dr. Afşin Sarıtaş. I would like to express my gratitude and deep appreciation to him for his guidance, positive suggestions and also for the great research environment he had provided.

I would like to thank my father, mother and brother for their love, understanding and encouragement throughout my life. This thesis is dedicated to them.

I would like to also express my thanks for his great friendship and assistance to Hakan Karaca.

Finally, I would like to give thanks to my love Gülru Göksüzoğlu for her invaluable support during this long period.

TABLE OF CONTENTS

ABSTRACT	iv
ÖZ.....	vi
ACKNOWLEDGEMENTS	ix
TABLE OF CONTENTS	x
LIST OF TABLES.....	xiii
LIST OF FIGURES	xiv
LIST OF SYMBOLS	xviii
CHAPTER	1
1. INTRODUCTION	1
1.1 GENERAL	1
1.2 PREVIOUS RESEARCH.....	5
1.2.1 Finite Element Models	5
1.2.2 Nonlinear Interaction in Frame-Walls.....	6
1.3 OBJECTIVES	8
1.4 ORGANIZATION	9
CHAPTER	10
2. MODELING AND ANALYZING FRAME ELEMENTS.....	10
2.1 INTRODUCTION.....	10
2.2 OPENSEES.....	11
2.2.1 Introduction.....	11
2.2.2 Tcl Command Language	12
2.2.3 Using Commands from Opensees.....	12
2.3 GEOMETRY OF THE STRUCTURAL FRAME	13
2.3.1 Geometry of Structural Frame without Shear Wall.....	13
2.3.2 Geometry of Structural Frame with Shear Wall.....	15
2.4 MODELING OF THE FRAME ELEMENTS	16

2.4.1 Information of Modeling Frame Elements	16
2.4.2 Modeling and Detailing of the Beams and Columns	17
2.4.3. Modeling of the Shear Walls	21
2.5 MATERIAL PROPERTIES	23
2.5.1 Steel	24
2.5.2 Concrete	25
CHAPTER	27
3. RESULTS AND DISCUSSION	27
3.1 ANALYSIS CASES OF THE FRAMES	27
3.2 STATIC PUSHOVER ANALYSIS	28
3.2.1 Structural Frame without Wall	28
3.2.1.1 Plastic Hinge Formation in the Structural Frame without Wall under Linear Geometry and $0.2N_o$ Axial Load	32
3.2.1.2 Plastic Hinge Formation in the Structural Frame without Wall under Nonlinear Geometry and $0.2N_o$ Axial Load	36
3.2.2 Frame–Wall Structure	39
3.2.2.1 Effect of Nonlinearity in the Wall	40
3.2.2.2 Influence of Axial Force in the Frame-Wall Structural System	41
3.2.2.3 Bending Moment Diagram and Curvature Distribution in the Walls of the Frame-Wall System	45
3.2.2.4 Load Redistribution due to Yielding in the Walls	47
3.3 NONLINEAR DYNAMIC ANALYSIS	51
3.3.1 Total Base Shear versus Drift Ratio of the Top Storey	53
3.3.2 Influence of Wall Stiffness	58
3.3.3 Comparison of Inter-Story Drift Ratios from Static Pushover and Nonlinear Dynamic Analyses	62
CHAPTER	65
4. CONCLUSIONS	65
4.1 SUMMARY	65
4.2 CONCLUSION	66

4.3 RECOMMENDATIONS FOR FUTURE RESEARCH	68
REFERENCE.....	69

LIST OF TABLES

TABLES

Table 3.1 – Comparison of the Results of the Frame–Wall System with Different Wall Lengths.....	44
Table 3.2 – The Characteristic of Earthquake Records	52

LIST OF FIGURES

FIGURES

Figure 1.1 – Plan View of the Floor of a Building	3
Figure 2.1 – Typical Floor Plan of a Structural Building	13
Figure 2.2 – Geometry of the Structural Frame without Shear Wall.....	14
Figure 2.3 – Geometry of the Structural Frame with Shear Wall (L=140cm)	15
Figure 2.4 – Cross-Sectional Dimensions of the Beams and Columns	18
Figure 2.5 – Reinforcement Details of the Beams and Columns	19
Figure 2.6 – Axial Force Bending Moment Interaction for Beam Section.....	20
Figure 2.7 – Axial Force Bending Moment Interaction for Column Section.....	20
Figure 2.8 – Cross-Sectional and Reinforcement Details of the Shear Wall	21
Figure 2.9 – Cross-Sectional and Reinforcement Details of the First Storey Wall	22
Figure 2.10 – Regions in the Shear Wall	23
Figure 2.11 – Stress-Strain Relation of Steel.....	25
Figure 2.12 – Stress-Strain Relation of Concrete under Compression	26
Figure 3.1 – Profile of Lateral Force Applied on the Building Structure	29
Figure 3.2 – Comparison of the Linear and Nonlinear Geometry in the Response of the Building without Wall (N=0.1No)	30
Figure 3.3 – Comparison of the Linear and Nonlinear Geometry in the Response of the Building without Wall (N=0.2No)	30

Figure 3.4 – Comparison of the Linear and Nonlinear Geometry in the Response of the Building without Wall ($N=0.3N_0$).....	31
Figure 3.5 – Hinge Formations for Structural Frame without Wall under $0.2N_0$ Axial Load and Linear Geometry	32
Figure 3.6 – Formation of Hinges on the Load-Displacement Plot of the Structural Frame without Wall under $0.2N_0$ Axial Load and Linear Geometry	33
Figure 3.7 – Moment vs. Curvature Relation for the Rightmost Column at First Storey	34
Figure 3.8 – Moment vs. Curvature Relation for the Rightmost Beam at First Floor	34
Figure 3.9 – Structural Frame without Wall under Linear Geometry	35
Figure 3.10 – Hinge Formations for Structural Frame without Wall under $0.2N_0$ Axial Load and Nonlinear Geometry	36
Figure 3.11 – Moment Curvature for Rightmost Column.....	37
Figure 3.12 – Moment Curvature for Rightmost Beam	38
Figure 3.13 – Structural Frame without Wall under Nonlinear Geometry.....	39
Figure 3.14 – Profile of Lateral Force Applied to the Building Structure	40
Figure 3.15 – Comparison of the Load-Displacement Responses of the Building without Wall and with Elastic and Inelastic Walls under Zero Axial Force	41
Figure 3.16 – Comparison of the Linear and Nonlinear Geometry in the Response of the Frame–Wall ($N=0.1N_0$).....	42
Figure 3.17 – Comparison of the Linear and Nonlinear Geometry in the Response of the Frame–Wall ($N=0.2N_0$).....	42
Figure 3.18 – Comparison of the Linear and Nonlinear Geometry in the Response of the Frame–Wall ($N=0.3N_0$).....	43
Figure 3.19 – Frame-Wall System with 140cm Wall Length	46
Figure 3.20 – Frame-Wall System with 250cm Wall Length	47

Figure 3.21 – Percentage of Shear Force Carried by Each Column/Wall (Wall Length=140 cm)	48
Figure 3.22 – Percentage of Shear Force Carried by Each Column/Wall (Wall Length=200 cm)	48
Figure 3.23 – Percentage of Shear Force Carried by Each Column/Wall (Wall Length=250 cm)	49
Figure 3.24 – Response of Frame-Walls with Different Wall Lengths under Zero Axial Force	51
Figure 3.25 – Total Base Shear vs. Time History for Chi-Chi Earthquake Record.....	53
Figure 3.26 – Total Base Shear vs. Time History for Coalinga Earthquake Record.....	54
Figure 3.27 – Total Base Shear vs. Time History for Erzincan Earthquake Record.....	54
Figure 3.28 – Global Drift Ratio vs Time History for Chi-Chi Earthquake Record.....	55
Figure 3.29 – Global Drift Ratio vs Time History for Coalinga Earthquake Record.....	56
Figure 3.30 – Global Drift Ratio vs Time History for Erzincan Earthquake	56
Figure 3.31 – Base Shear Force vs. Time History for Chi-Chi Earthquake Record.....	59
Figure 3.32 – Base Shear Force vs. Time History for Coalinga Earthquake Record.....	59
Figure 3.33 – Base Shear Force vs. Time History for Erzincan Earthquake Record.....	60
Figure 3.34 – Global Drift Ratio vs. Time History for Chi-Chi Earthquake Record.....	61
Figure 3.35 – Global Drift Ratio vs. Time History for Coalinga Earthquake Record.....	61

Figure 3.36 – Global Drift Ratio vs. Time History for Erzincan Earthquake Record.....	62
Figure 3.37 – Comparison of the Inter-storey Drifts from Erzincan Earthquake Results and the Pushover Analysis Results of the Frame without Wall System	63
Figure 3.38 – Comparison of the Inter-storey Drifts from Coalinga Earthquake Results and the Pushover Analysis Results of the Frame without Wall System	64

LIST OF SYMBOLS

A_c = Gross area of column cross-section

A_{st} = Total cross sectional area of longitudinal reinforcement in column

f_{ck} = Characteristic compressive strength of concrete

f_{ctd} = Design tensile strength of concrete

f_{yk} = Characteristic yield strength of the longitudinal reinforcement

f_{yd} = Design yield strength of the longitudinal reinforcement

H_{cr} = Critical height of shear wall

H_w = Total height of shear wall from basement to top level

L_u = Length of boundary zone along critical height of shear wall

L_w = Length of shear wall

N_o = Axial load capacity

ρ = Ratio of tension reinforcement in a beam section

ρ' = Ratio of compression reinforcement in a beam section

CHAPTER 1

INTRODUCTION

1.1 GENERAL

Reinforced concrete (RC) buildings with structural walls have shown superior seismic performance in the earthquakes of the last three decades. Experiences from past earthquakes clearly indicate that the installation of structural walls increases the overall rigidity of buildings, thereby reducing seismic distortion. Despite the known superiority of frame-wall type structures, until the 1980s, engineers and researchers in United States, Japan, New Zealand and other countries gave preference to moment resisting frames, mainly due to a lack of understanding of the inelastic behavior of frame-wall structures under strong earthquakes (Fintel 1995).

In performance-based earthquake engineering, a structural system should have sufficient strength to limit damage during minor earthquakes, and it is expected to maintain a level of strength under increased deformation demands (ductility) during strong seismic excitations. For the latter case, damage is only acceptable as long as sufficient energy dissipation is provided in this process. For this reason, structural members of a building are designed to yield in flexure, where this failure

mode should provide the required ductility and energy dissipation during earthquake loadings to these members, and shear failure is prohibited due to the brittle nature of the response.

Structural walls, which are also called shear walls, provide the needed resistance to lateral loads when they are placed at certain convenient and strategic locations in a building. Such walls are in effect deep vertical cantilever beams that provide lateral stability to structures (Murty 2005). Shear walls in earthquake resistant buildings control lateral drift thereby reduce damage to both structural elements such as the columns and the non-structural elements.

Structural walls are designed for strength, stiffness and ductility in order to prevent structural collapse in a major earthquake. They behave elastically during minor earthquakes. On the other hand, they may no longer remain elastic under strong ground motions, thus the design force requirements of buildings with walls are thus reduced because of yielding and subsequent energy dissipation in the lateral load resisting system. If the structural wall can develop the required ductility, the requirement for both strength and stiffness in the structure are satisfied (Paulay and Priestley 1992).

The plan view of a floor of a building that is subjected to lateral forces is shown in Figure 1.1, where these forces are assumed to be applied at each floor. When lateral forces act in shown direction, the slabs and the beams of the floor transfer these loads mainly to the shear walls A and B, as well as the columns of the frame system. If the forces are applied from the other direction the loads will be transferred mainly to the shear walls C and D. Biaxial application of the lateral force actually necessitates the concentric distribution of wall stiffness and the mass at a floor in the

building as close as possible, otherwise torsional effects would need to be considered in the response.

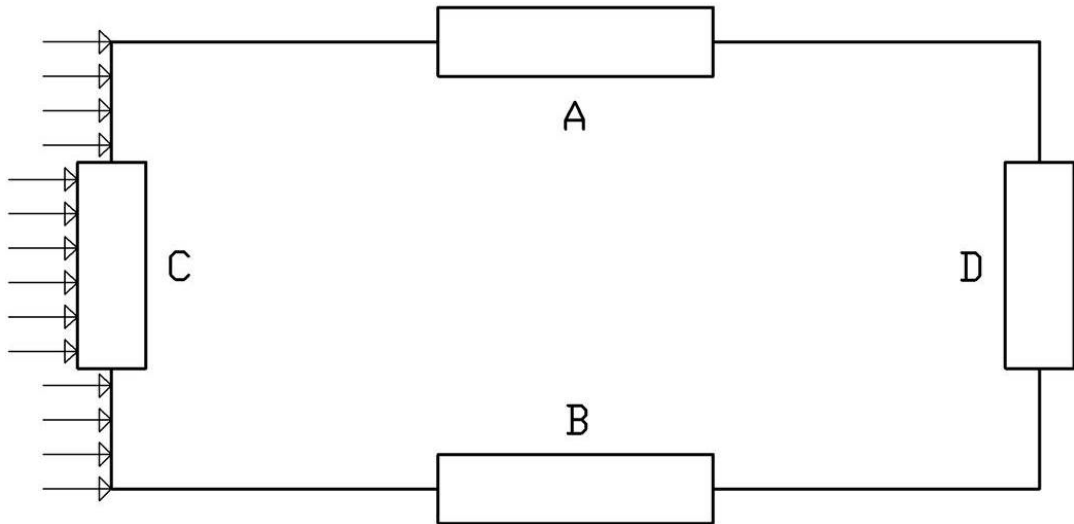


Figure 1.1 – Plan View of the Floor of a Building

The two most important factors in the analysis and design of building structures are choosing an appropriate structural model that reflects the actual behavior of the system and deciding on the analysis technique to be performed on the structure. The model must represent the changes in stiffness, strength, deformation capacity of members with sufficient accuracy. Analysis methods are usually the same for both 2-d and 3-d models. In this thesis a 2-d model is considered, which is sufficient for buildings with regular configuration and minimal torsion.

In practical engineering, structural analysis of a reinforced concrete building with or without shear wall is generally performed in the elastic range. For actual cases, the behavior of structural system can be in the nonlinear range; thus during the last two decades, analysis and design of

building structures have started to take into account the nonlinear range of response.

Influence of material and geometric nonlinearities occurring in the beams, columns and walls of a building creates an interaction between the wall and the frame system. Investigation of this interaction requires the use of advanced frame finite element models that consider the spread of inelasticity over a member's span, the interaction of forces at a section, as well as the influence of axial force on the stiffness and strength of a member.

Several computer programs are developed to investigate the behavior of building structures in the nonlinear range by considering material and geometric effects to various extents. To this end, Open System for Earthquake Engineering Simulation (OpenSees) program developed by McKenna et al. (1999) will be utilized in this thesis. OpenSees is selected for its vast library of constitutive, finite element models as well as solution strategies for performing static and dynamic nonlinear analysis. Force formulation frame elements developed by Spacone et al. (1996) are used in this thesis for modelling the inelastic action spread over the entire length of each beam, column and wall. The coupling of the section forces is obtained by the fibre discretization of the section into several material points, thus a realistic coupling of internal forces is obtained. Each section is divided into confined and unconfined regions and appropriate material properties are used for concrete and steel for the simulation of cyclic loading. Shear deformations in the wall are assumed to remain in the elastic range; thus the walls do not fail in shear. Nonlinear geometric effects are considered through corotational formulation implemented in OpenSees by de Souza (2000). Both static pushover and dynamic analyses are performed in order to replicate the worst case scenario for a possible earthquake.

In the following we present previous research on the study of inelastic modeling of structural walls and the inelastic interaction in frame-wall systems.

1.2 PREVIOUS RESEARCH

The following literature review is divided into two parts. First, the finite element models on beams, columns and walls are presented, and then the research work considering the interaction of material and geometric nonlinearities in frame-wall type structures are presented.

1.2.1 Finite Element Models

Most of the beam and column finite element models consider plasticity as lumped at the ends of members and basically follow the one component approach of an elastic beam with nonlinear end hinges of Giberson (1967). These models are specifically calibrated to match the load-deformation responses from experimental data. It is important to know that the experimental loading and boundary conditions are unique and do not represent the varying conditions in a building. In addition to this limitation, evolution of the response of a yielding member also requires close attention, and several assumptions are further introduced to the models. A detailed literature review of these models is presented by Saritas (2006).

In the last decade, the use of spread inelasticity elements with fiber discretization of the section has gained popularity, since a realistic coupling of the section forces is easily attainable through this method. Accuracy problems faced in displacement-based elements are overcome by the use of hybrid/mixed formulation. The advantages of using mixed

methods are presented by Taylor et al. (2003). Spacone et al. (1996) developed a force formulation element from this approach. In a nonlinear frame element, coupling of section forces with fiber discretization is achieved by using either uniaxial or multiaxial constitutive models at each material point on the section.

The use of frame finite elements is less common in RC shear walls. Simple models similar to the lumped approach were initially considered for capturing nonlinearities in walls. Vulcano and Bertero (1987) used such an approach to idealize the wall with three vertical line elements. Orakcal and Wallace (2004) improved on this model for the study of flexural response of rectangular and T-shaped walls. Ghobarah and Youssef (1999) developed a macro model that represents the behavior of structural walls comprising of four steel springs, four concrete springs and a shear spring connected by rigid bars and truss elements.

Besides these macro approaches, there have been successful attempts in capturing flexural yielding behavior of walls with spread inelasticity elements and fiber discretization, as well. A displacement-based approach was presented by Kotronis and Mazars (2005), which required several element discretization per span in order to obtain an accurate response. A mixed formulation frame element model is recently developed by Saritas (2006) and considers the interaction of axial force, shear force and bending moment at a section over wall's span.

1.2.2 Nonlinear Interaction in Frame-Walls

Inelastic behavior of RC frame-wall structures was considered in the past by Clark (1968) under the supervision of J.G. MacGregor. Clark considered both material and geometric nonlinearities through the use of

lumped plasticity models with idealized elasto-plastic moment curvature relations. For their analysis, they selected a twenty-storey two-bay RC structure, and studied the effect of finite width of walls, effect of shear wall stiffness, and axial shortening of columns on the structure's response. Katusuhiko and Schnobrich (1981) only considered material nonlinearity, again through the use of simple models. Kayal (1985) employed a simplified elastic analysis of a building, and studied nonlinear interaction phenomenon in RC frame-wall systems. In his model, Kayal substituted the building with a single column element and wall element connected through a link, and attached a nonlinear spring to the column to consider nonlinear material behavior. He studied the presence of combined vertical and lateral loading for different ratios of beam-to-column stiffness, column-to-wall stiffness, slenderness ratio of columns, and the proportion of lateral to vertical load ratio.

Kongoli et al. (1999) investigated the effect of the structural walls on the elastic-plastic response of short to medium-height frame-wall buildings. They used a single bay building with independent lumped mass systems to represent frames and walls joined at each floor. The base was assumed to be fixed for both the frames and walls. A series of shear springs were used to model the possibility of shear failure in walls. The inelastic flexural behavior in the walls was considered through the use of lumped spring model by Takayanagi (1976). In their study, geometric nonlinear effects were ignored. They concluded that shear failure in walls should be eliminated in order to decrease plastic displacements. They have also established empirical relations between base shear coefficients of the frames and walls in terms of peak ground accelerations.

Akış (2004) modeled and analyzed frame-wall structures under both static and dynamic loads, where only elastic analysis was performed

without the consideration of material and geometric nonlinear effects. Elastic frame elements were utilized in modeling the shear walls. Each shear wall was replaced by an idealized frame structure consisting of a column and rigid beams located at floor levels. Static pushover analysis, response spectrum analysis and time history analysis were performed through the use of SAP2000 and ETABS computer programs. The results obtained from analysis were compared with several methods and experimental results taken from literature.

1.3 OBJECTIVES

This research focuses on the analytical investigation of the material and geometric nonlinear effects in frame-wall structures by using spread plasticity frame element models and fiber discretization of section. Both static pushover and nonlinear dynamic analyses will be performed to study the interaction of the frame and wall system and the force redistributions occurring as a result of yielding in the members.

The objectives of this thesis are:

- To observe the effect of linear and nonlinear geometry in buildings without walls and frame-wall structures by performing static pushover analysis under various levels of axial force.
- To investigate the influence of the inelastic material behavior in shear walls on the frame-wall system through both static pushover and dynamic analyses under lateral forces and several earthquake motions.

- To search the effect of change in the stiffness of the wall to the overall response of the structure.

1.4 ORGANIZATION

This thesis is organized into four chapters as follows:

Chapter 2 starts with the description of the computer program used in this study. This is followed by the description of the geometry of the structural frame with and without walls. The chapter then gives information about the modeling and detailing of the beam, column and shear wall members. The chapter concludes with the given details of the material properties.

In Chapter 3, the three analysis cases of the frames are presented at the beginning. Pushover and dynamic analyses are performed on the structural systems in the rest of this chapter.

Chapter 4 provides the summary and conclusion of the work, and recommendations for future research.

CHAPTER 2

MODELING AND ANALYZING FRAME ELEMENTS

2.1 INTRODUCTION

There are two important factors in the analysis and design of structures. First one is choosing a realistic structural model replicating the actual behavior of the system as close as possible and the other one is choosing an analysis technique to be carried out on the model structure.

In the first part of this chapter, general information is given on OpenSees finite element program, which is used to analyze the building structures in this thesis. Geometry of the selected structural frames is introduced in the second part of this chapter, then the modeling of structural elements as beam, column and shear wall are presented. Finally, the material properties and the selected material models are described.

2.2 OPENSEES

2.2.1 Introduction

Modern earthquake engineering utilizes modeling and simulation to understand the behavior and performance of systems during earthquakes. With the support of the National Science Foundation, Pacific Earthquake Engineering Research Center developed the Open System for Earthquake Engineering Simulation, OpenSees for short, as a software platform for research and application of simulation for structural and geotechnical systems. OpenSees software framework uses object-oriented methodologies to maximize modularity and extensibility for implementing models for behavior, solution methods, and data processing and communication procedures. The framework is a set of inter-related classes, such as domains (data structures), models, elements (which are hierarchical), solution algorithms, integrators, equation solvers, and databases (McKenna et al. 1999).

The software architecture and open-source approach for OpenSees provide many benefits to users interested in advanced simulation of structural and geotechnical systems with realistic models of nonlinear behavior. First, the modeling approach is very flexible in that allows selection and various combinations of a number of different element formulations and material formulations, along with different approximations of kinematics to account for large-displacements and P- Δ effects. As an open-source project, developers and researchers are using the extensible features of the software architecture to add additional capability. A second advantage is that there is a wide range of solution procedures and algorithms that the user can adapt to solve difficult nonlinear problems for static and dynamic loads. Finally, another

feature is that OpenSees has a fully programmable scripting language (Tcl) for defining models and solution procedures.

2.2.2 Tcl Command Language

Tcl is a string-based scripting language and interpreter which was first designed by John Ousterhout. It was designed for easy learning, but it should provide all the powerful functions the expert programmer wants. It is popular for prototyping, scripting and easy testing.

The Tcl scripting language was selected to support the OpenSees commands, which are used to define the problem geometry, loading, formulation and solution. Some useful programming tools are provided by the Tcl language such as variables manipulation and control structures.

2.2.3 Using Commands from Opensees

The seismic response analysis platform selected for the simulation studies is OpenSees. This selection was based on the convenience of the program for seismic response simulations and the suitable modeling elements in its library.

Nonlinear beam-column elements and fiber sections are utilized to model structural frame elements which are beam, column and shear wall in OpenSees. Static pushover and dynamic ground motion analyses are considered in frame analysis. To observe the rigid end-zone effects, the linear transformation command was used. Moreover, corotational command was used to monitor its effects on the results. Corotational geometric transformation is implemented in OpenSees by de Souza

(2000), and provides better convergence rate than P- Δ geometric transformation in the solution of structural problems.

2.3 GEOMETRY OF THE STRUCTURAL FRAME

2.3.1 Geometry of Structural Frame without Shear Wall

The floor plan view of the building without wall is presented in Figure 2.1, where the centerline to centerline distance between each column is 5 m. The frame at A-A axis of the building is considered for analysis in this thesis, and geometry of the frame is shown in Figure 2.2.

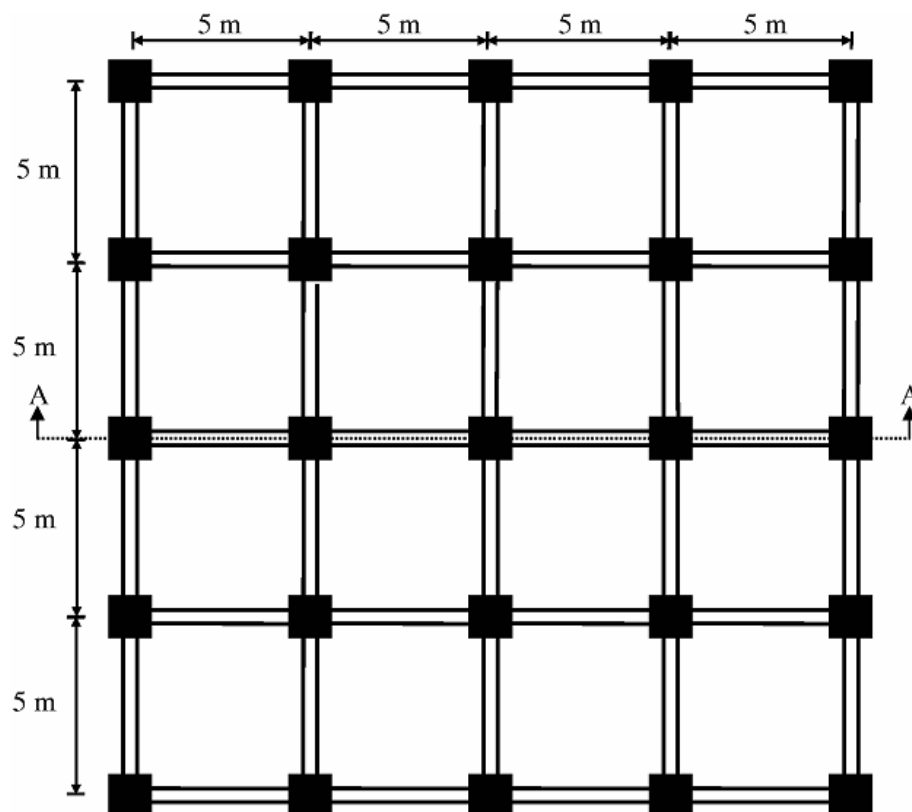


Figure 2.1 – Typical Floor Plan of a Structural Building

The 2-d structural frame without shear wall is four stories tall with a total height of 12 meters, and there are 4-bays with a total length of 20 meters as shown in Figure 2.2. This structure represents a typical low-rise residential building in an area of high seismicity.

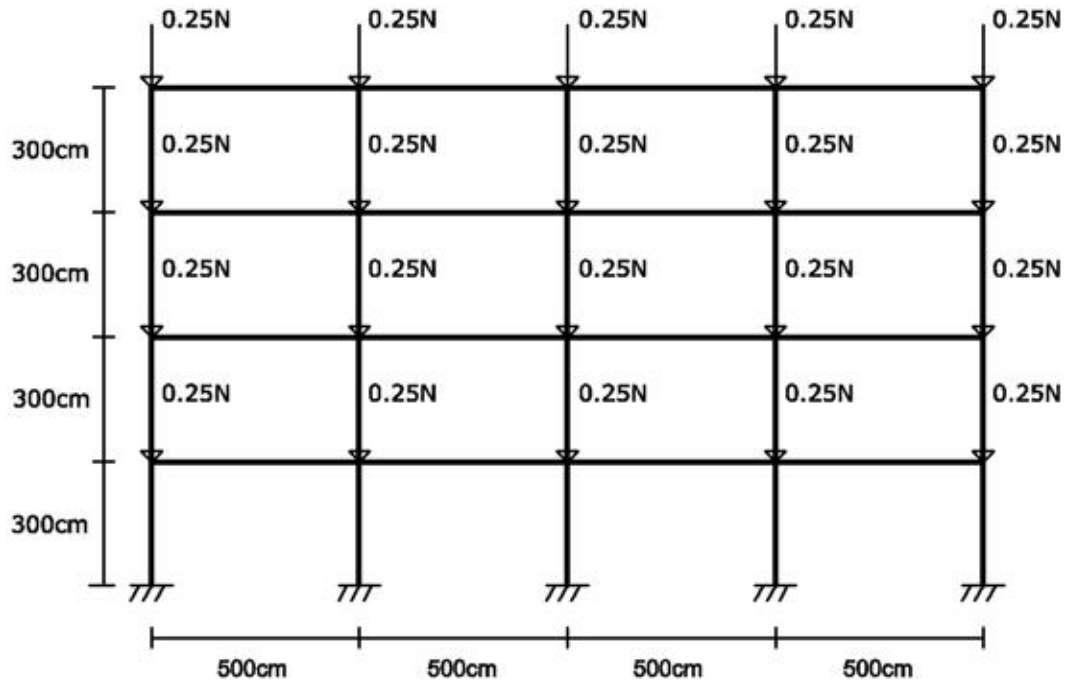


Figure 2.2 – Geometry of the Structural Frame without Shear Wall

The total dead weight of the beams and columns of the structural frame without wall in Figure 2.2 is equal to 51725.30 kg (51.73 ton). The contribution of dead weight from slabs is calculated for a clear span of 5 m as shown in Figure 2.1 and for a minimum slab thickness of 12 cm, and it is equal to 115200 kg (115.20 ton).. In this calculation, the mass density of concrete and steel are taken as 2400 kg/m^3 and 7850 kg/m^3 , respectively

2.3.2 Geometry of Structural Frame with Shear Wall

The column at the axis of symmetry is replaced with a shear wall in Figure 2.2, and the frame-wall structural system in Figure 2.3 is obtained. In the analysis, the length of the wall is considered as 140 cm, 200 cm, and 250 cm in order to study the influence of wall stiffness on the response.

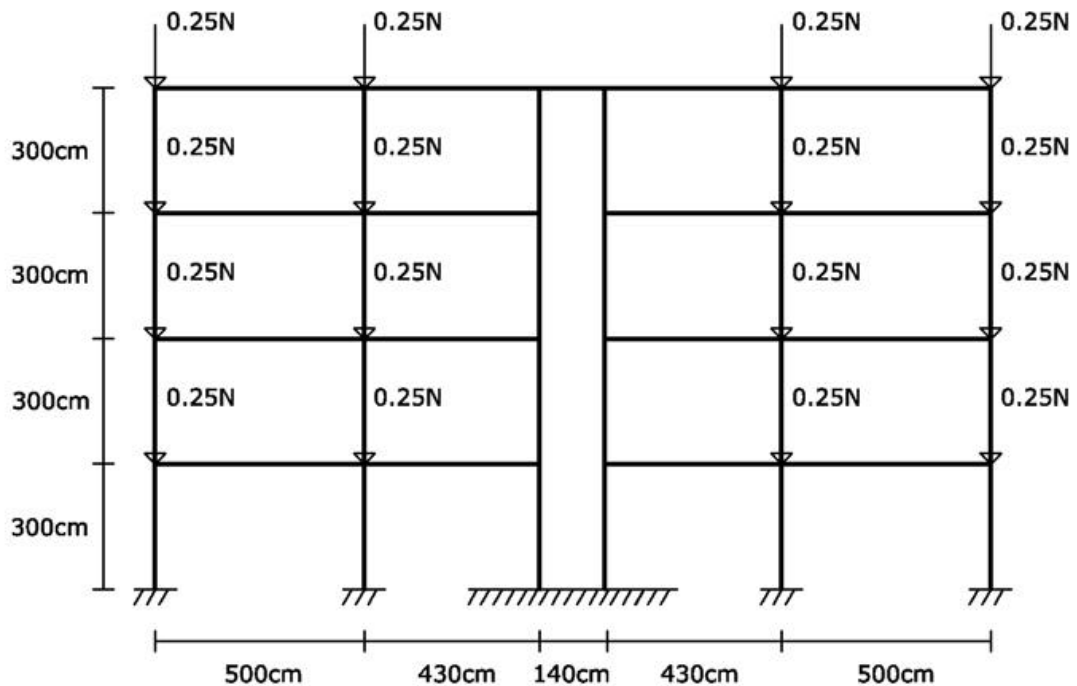


Figure 2.3 – Geometry of the Structural Frame with Shear Wall (L=140cm)

The total dead weight of the beams, columns and walls of the frame-wall structure with 140cm wall length is 54071.75 kg (54.07 ton). The contribution of dead weight from slabs is calculated for a clear span of 5 m and for a minimum slab thickness of 12 cm, and it is equal to 115200 kg (115.20 ton).

2.4 MODELING OF THE FRAME ELEMENTS

2.4.1 Information of Modeling Frame Elements

Buildings should be designed like a ductile chain. For example, consider a common urban residential apartment construction, i.e. a multi-storey building made of reinforced concrete. It consists of horizontal and vertical members, namely beams and columns. The seismic inertia forces generated at floor levels are transferred through the beams and columns to the ground. The correct building components need to be made ductile. The failure of a column can affect the stability of the whole building, but the failure of a beam causes localized effect. Therefore, it is better to make beams to be the ductile weak links than columns. This method of designing RC buildings is called the strong column weak beam design method. In this thesis, strong column weak beam design method is considered for the design of structural frame elements.

Nonlinear beam column element is used to construct a nonlinear beam column object in OpenSees, and this element considers the spread of plasticity along its length. This beam-column element model was originally proposed by Spacone et al. (1996). The fiber discretization of the cross section allows for the interaction of the axial force and bending moment to be rationally accounted for.

A fiber section has a general geometric configuration formed by sub-regions of simpler, regular shapes like quadrilateral, circular and triangular regions called patches. In addition, layers of reinforcement bars can be specified. The subcommands patch and layer like circular layer command and straight layer command are used to define the discretization of the section into fibers.

Uniaxial Material objects are created to define the fiber stress-strain relationships for the following: confined concrete in the column core, unconfined concrete in the column cover, and the reinforcing steel.

To achieve more precise results, five integration points corresponding to Gauss-Lobatto quadrature rule are used for each element that exhibits nonlinear action in the study.

2.4.2 Modeling and Detailing of the Beams and Columns

The dimensions of the beam section in this thesis are assumed as follows: section depth 50 cm, width 30 cm, and concrete cover 3 cm. The dimensions of the column section are taken as follows: the section depth and width are 40 cm each, and the concrete cover is 3 cm. The geometry of the beam and column sections is presented in Figure 2.4, where the axis of bending in analysis will be z-axis. These dimensions comply with the requirements of Turkish Earthquake Code 2007 (TEC 2007).

The beam and column sections are separated into confined and unconfined concrete regions as shown in Figure 2.4, for which separate fiber discretizations will be generated in OpenSees. Reinforcing steel bars will be placed between the boundary of the confined and unconfined regions.

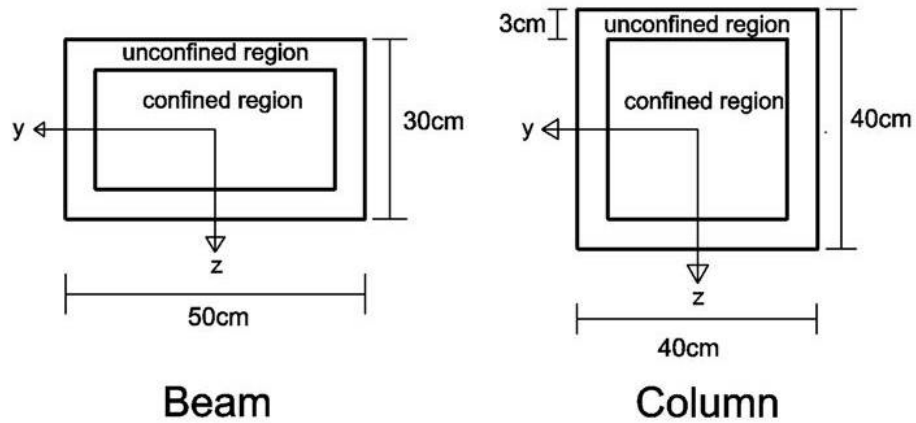


Figure 2.4 – Cross-Sectional Dimensions of the Beams and Columns

According to TEC 2007, the amount of tensile reinforcement ratio for a beam should be greater than $0.8 \cdot f_{ctd} / f_{yd}$ and not exceed 2% and the maximum value calculated from the Turkish Standard Code TS-500. In this study, the amount of top and bottom reinforcement ratios of each beam are taken in accordance with these limitations as 1% each. According to TEC 2007, the amount of reinforcement ratio in a column should not be less than 1% and not be greater than 4% of the total cross-section area. In this study, this ratio is chosen as 3%. The reinforcement details of the beam and column sections are presented in Figure 2.5. These selected values result in a strong column and weak beam condition at each joint.

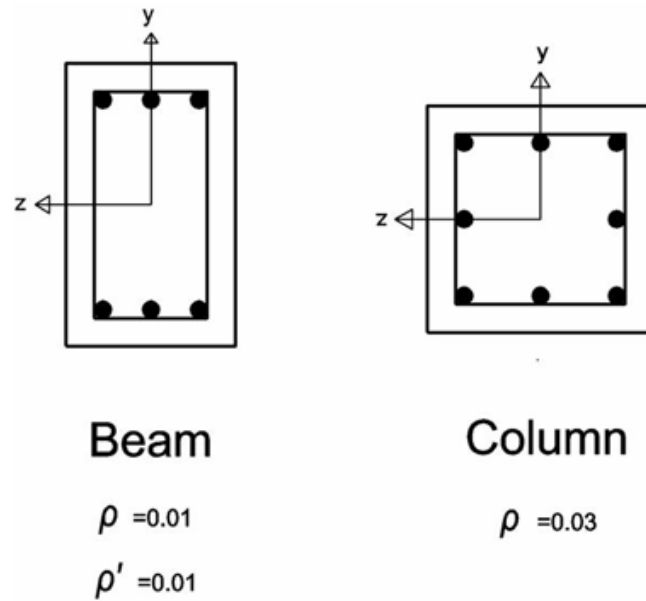


Figure 2.5 – Reinforcement Details of the Beams and Columns

The axial force bending moment interaction diagrams for above beam and column sections are presented in Figures 2.6 and 2.7, respectively. The bending moment capacity of the column section under zero axial force is 1.2 times of the bending moment capacity of the beam section under zero axial force. It is important to emphasize that the strength ratio between the moment capacity of the column and beam sections increases further as a result of the application of gravity loads.

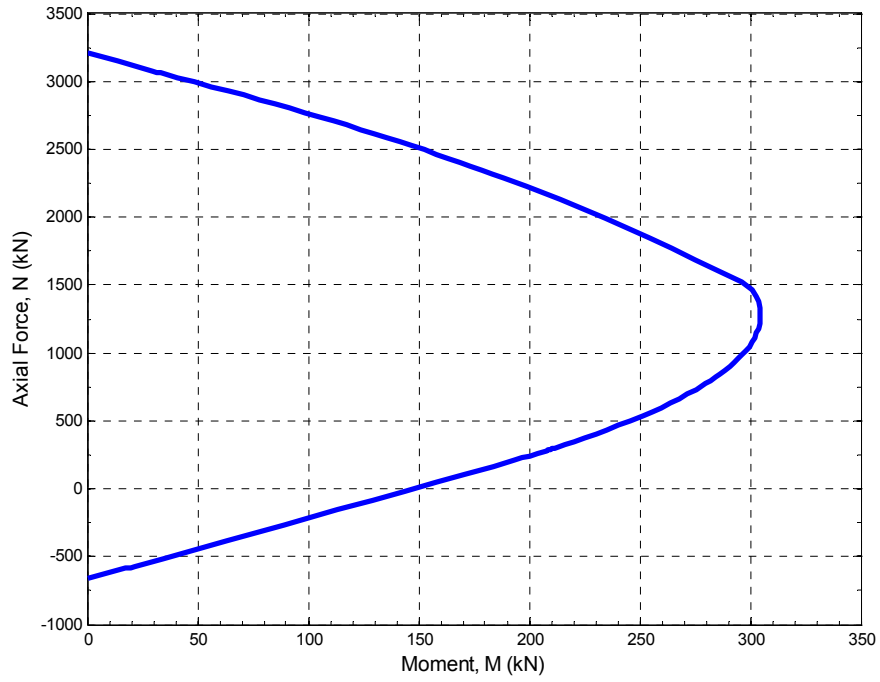


Figure 2.6 – Axial Force Bending Moment Interaction for Beam Section

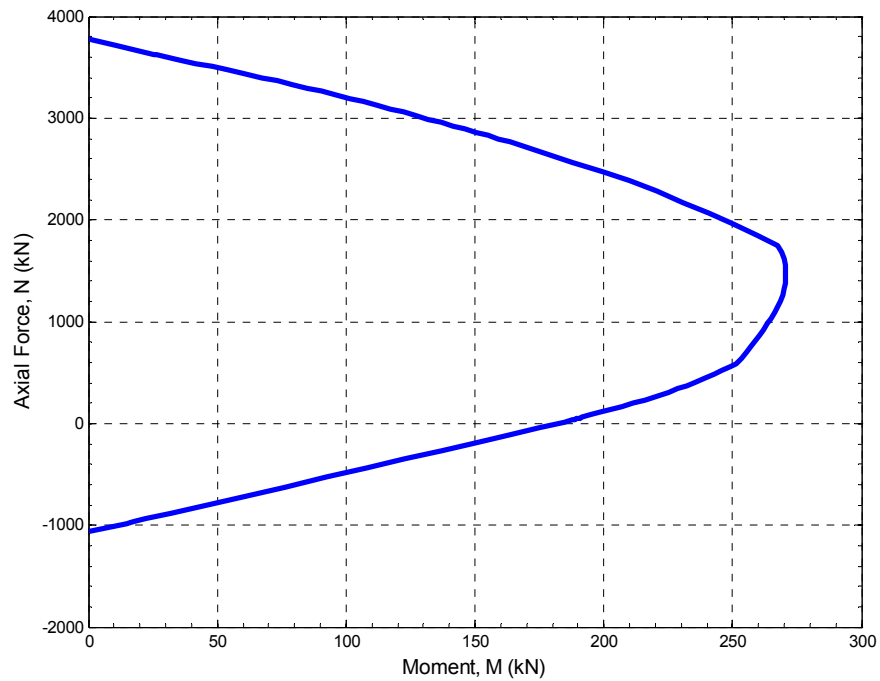


Figure 2.7 – Axial Force Bending Moment Interaction for Column Section

2.4.3. Modeling of the Shear Walls

The overall geometry and the layout of the shear wall sections are shown in Figure 2.8. According to TEC 2007, the ratio of the section length to thickness of a wall should be greater than 7, and the minimum thickness should be 20 cm.

In this study, three different levels of wall lengths are considered for a minimum wall thickness of 20 cm: these are 140 cm, 200 cm and 250 cm section lengths. For each case, a 2 cm of cover concrete is considered.

The wall section is separated into confined and unconfined concrete regions, for which separate fiber discretizations are generated. Some of reinforcing steel bars is placed between the boundary of the confined and unconfined regions and the others are placed in the unconfined regions (see Figure 2.8).

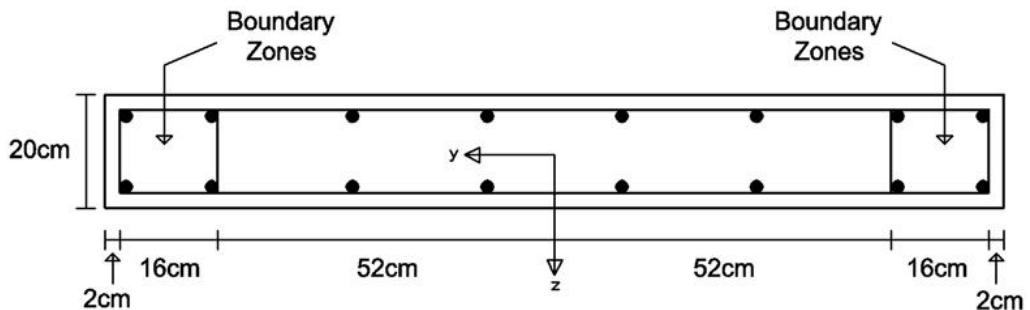


Figure 2.8 – Cross-Sectional and Reinforcement Details of the Shear Wall

Critical height of a shear wall (H_{cr}) is calculated in equation (1) according to TEC 2007.

$$\begin{aligned} H_{cr} &\geq L_w \\ H_{cr} &\geq H_w/6 \end{aligned} \quad (1)$$

For our structure with total wall height of 12 m, the second relation in Equation 1 gives H_{cr} equal to 200cm. For modeling of the frame-wall in this study, H_{cr} is taken 300cm (first storey), and the boundary zones of the first storey wall, which is seen in Figure 2.9 comply with the requirements provided in equation (2) according to TEC 2007.

$$\begin{aligned} L_u &\geq 2 \cdot b_w \\ L_u &\geq 2 \cdot L_w \end{aligned} \quad (2)$$

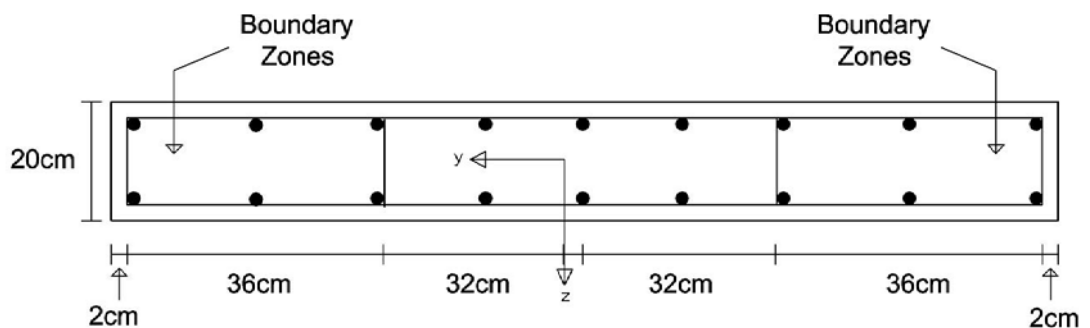


Figure 2.9 – Cross-Sectional and Reinforcement Details of the First Storey Wall

The regions in a shear wall section are shown in Figure 2.10. The main objective of defining different regions for the wall element is to create boundary zones that are confined by reinforcement at each end of the wall, an unconfined central part and cover regions.

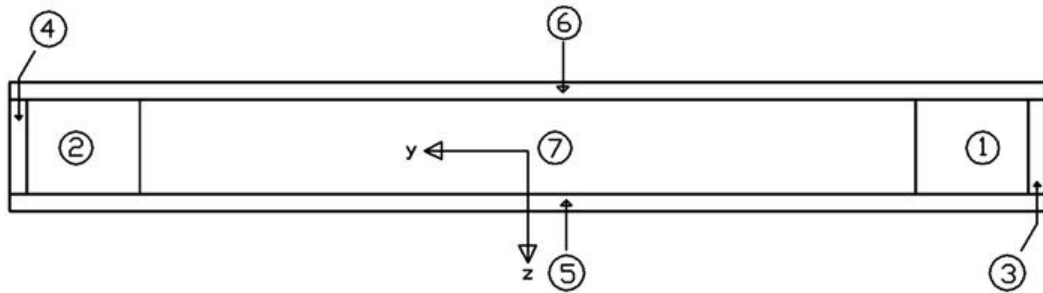


Figure 2.10 – Regions in the Shear Wall

According to TEC 2007, amount of web reinforcement ratio in a wall should not be less than 0.25% of the total web cross-section area, and the amount of reinforcement ratio in boundary zones of a wall should not be less than 0.1% of the total cross-section area. In this study, selected values for these ratios are taken greater than the minimum requirements.

Attention paid to the minimum reinforcement requirements when the length of the shear wall is increased to 200 cm and 250 cm. As the length of the wall increases, the reinforcement in the central unconfined region increases at the same time to satisfy the 20 cm spacing requirements. In addition, there isn't any change of the reinforcement in the boundary zones, since the length of this region stayed constant.

2.5 MATERIAL PROPERTIES

The concrete has a cylinder compressive strength of 20 MPa for all beams, columns and shear walls in the frame. The strain at maximum compressive strength is set to 0.002, the ultimate strain, i.e. the strain at which the compressive stress drops to zero is assumed as 0.006 for the

cover concrete region of all beams, columns and walls. The ultimate strain for the central part of the walls is taken as 0.008. Furthermore, the ultimate strain is chosen as 0.012 for all beams, columns and shear walls in the confined region. Young modulus and yield strength of steel are assumed as 200 GPa and 220 MPa, respectively.

2.5.1 Steel

The stress–strain curves for steel are generally assumed to be identical in tension and compression. For simplicity in calculations, it is necessary to idealize the one-dimensional stress–strain curve of steel. In this study, the material model for the reinforcing steel is taken as the GMP model. This model was first developed by Menegetto and Pinto (1973), and later revised in its current form by Filippou (1983). The parameter b in Figure 2.11 denotes the strain-hardening ratio of the second asymptote with respect to the first one and parameter R_0 controls the curvature of the transition from the elastic to the plastic-hardening branch. This model has a nonlinear behavior with the inclusion of Bauschinger effect for steel.

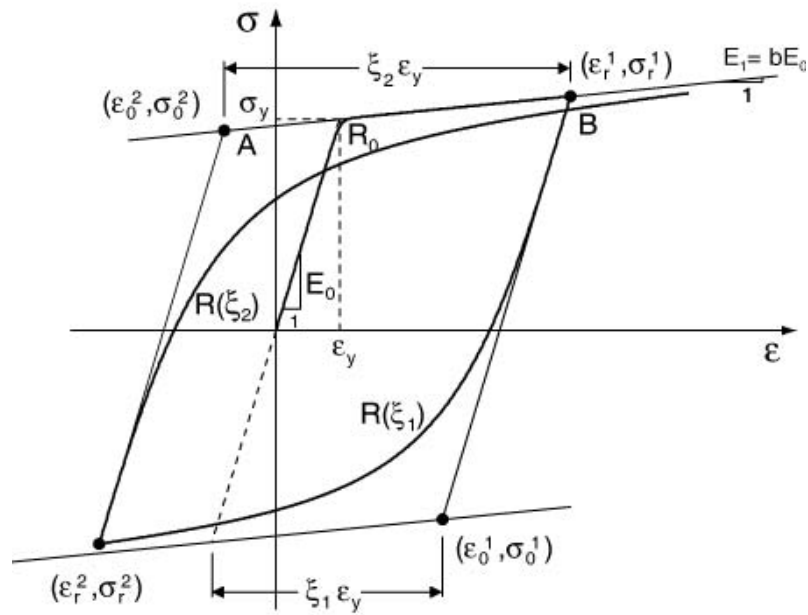


Figure 2.11 – Stress-Strain Relation of Steel

2.5.2 Concrete

The uniaxial concrete material model by Kent and Park (1971) is used for the concrete layers of the sections. The cyclic behavior of this model includes a degraded linear unloading/reloading stiffness proposed by Karsan and Jirsa (1969). There is no tensile strength of concrete in this model. The stress-strain diagram in compression consists of an ascending parabolic branch and a descending linear part for strains greater than the corresponding strain at peak stress. The parameter κ in Figure 2.12 is a coefficient that accounts for the volumetric confinement ratio and is equal to 1 for unconfined concrete. The parameter Z_m defines the strain softening slope and depends on κ .

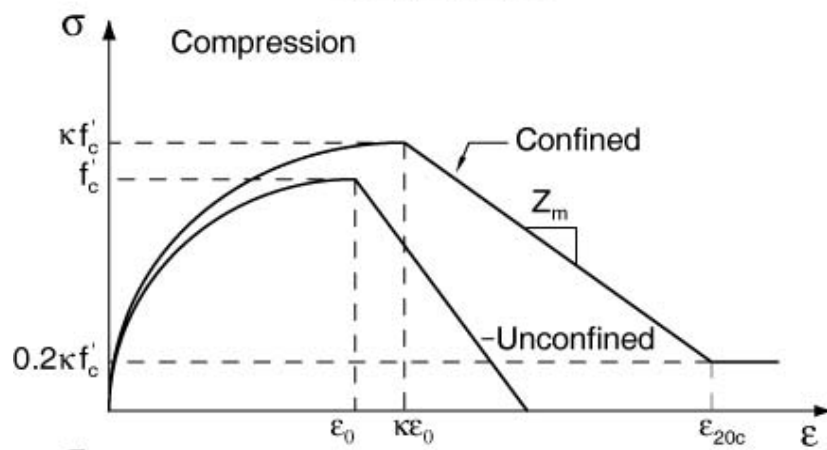


Figure 2.12 – Stress-Strain Relation of Concrete under Compression

CHAPTER 3

RESULTS AND DISCUSSION

There are two main analysis techniques used in this thesis namely static pushover and nonlinear dynamic analyses. Nonlinear geometric effects were only studied through static pushover analysis.

The considered classifications of the structure and loading conditions are explained in the first part of this chapter. Then static pushover analysis is performed for these cases in the second part. In the last part of this chapter, nonlinear dynamic analysis is performed through the use of various ground motion data.

3.1 ANALYSIS CASES OF THE FRAMES

Case 1: Static pushover analysis of the structural frame without shear wall in Figure 2.2 is pursued first under zero axial force. Then, the applied axial force at the very top columns is increased in order to study its effect on the load-deformation response of the structure under linear and nonlinear geometry.

Case 2: The influence of inelastic behavior of the wall to the overall response of the structure is pursued through static pushover analysis.

First, each wall is considered linear elastic, then nonlinear as described in Section 2.4. For this analysis, effect of axial force on the overall structural response is pursued through linear and nonlinear geometric analysis. Finally, the effect of change in the stiffness of the wall to the overall response of the structure is studied.

Case 3: Nonlinear dynamic analysis is performed using different earthquake data on the model defined in Chapter 2, where the geometric and material properties were documented in detail. And then the variation in the response of the structure under each earthquake data is investigated for the building with and without shear wall.

3.2 STATIC PUSHOVER ANALYSIS

3.2.1 Structural Frame without Wall

The beams and columns of the structural frame without shear wall are modeled as described in Chapter 2, where the geometric and material properties were documented in detail.

A lateral force profile as shown in Figure 3.1 is applied to the frame, where the axial force applied at the top of each column is 0.25 N. As a result, the axial force at first story columns is equal to N under pure gravity loading. The axial force N is first taken as zero, and then it is changed with respect to the axial load carrying capacity of the columns as calculated below where no strength reduction factor is considered.

$$N_o = f_{ck} (A_c - A_{st}) + A_{st} f_{yk} \quad (3)$$

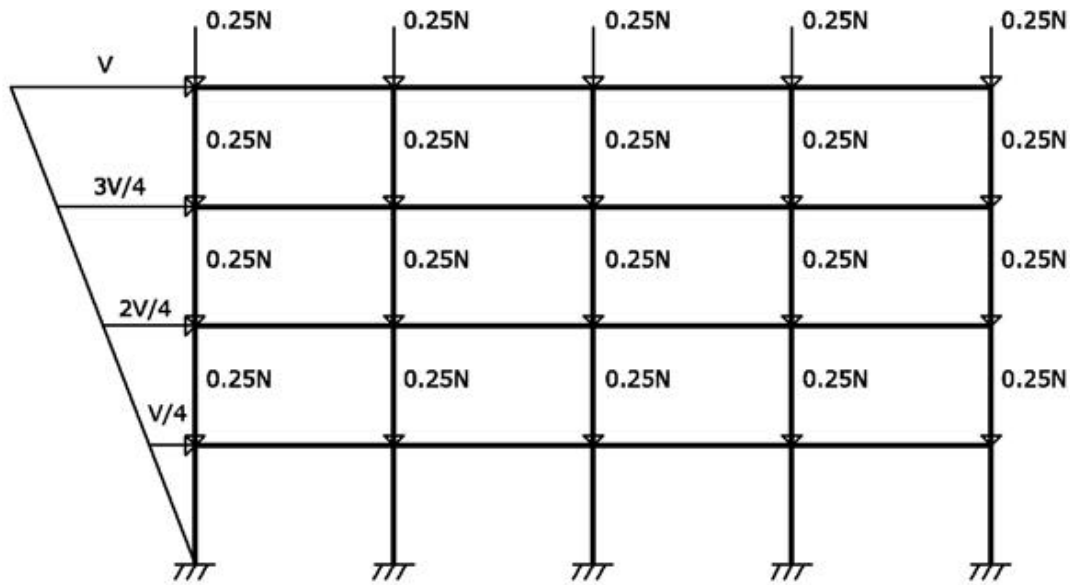


Figure 3.1 – Profile of Lateral Force Applied on the Building Structure

The axial force N is taken as: $0.1N_0$, $0.2N_0$ and $0.3N_0$. The results of the pushover analysis of the structural frame without wall under varying levels of applied axial force are presented in the following figures, where the influence of axial force under both linear and nonlinear geometry is investigated.

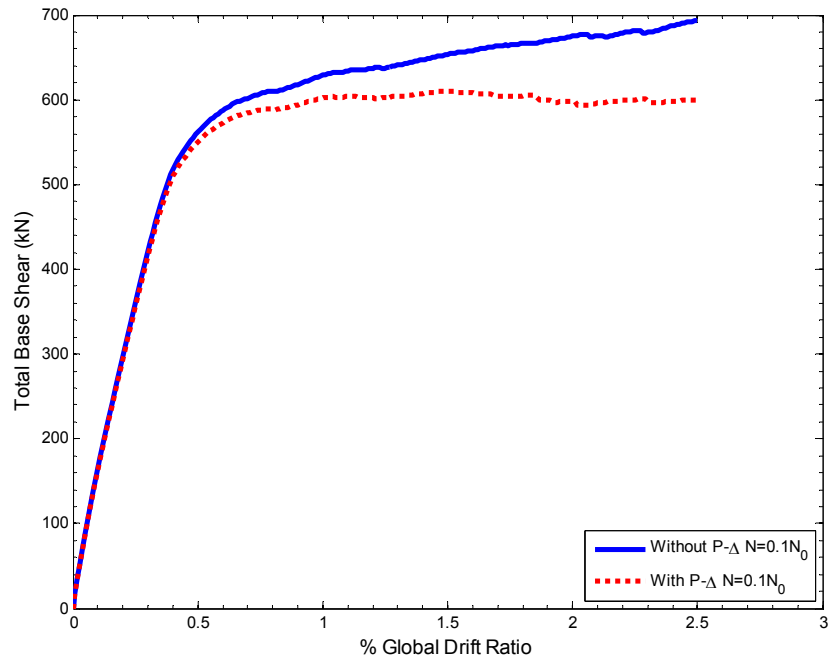


Figure 3.2 – Comparison of the Linear and Nonlinear Geometry in the Response of the Building without Wall ($N=0.1N_0$)

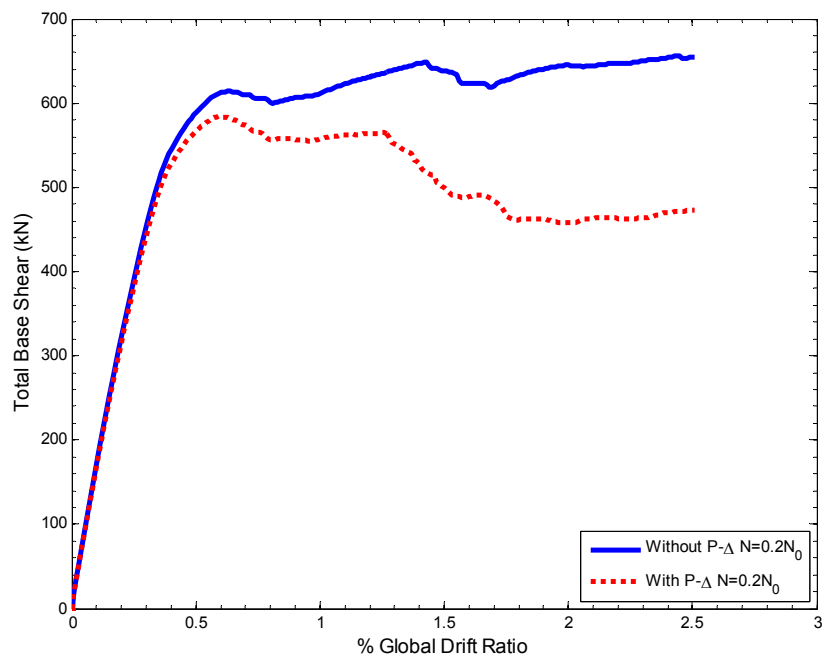


Figure 3.3 – Comparison of the Linear and Nonlinear Geometry in the Response of the Building without Wall ($N=0.2N_0$)

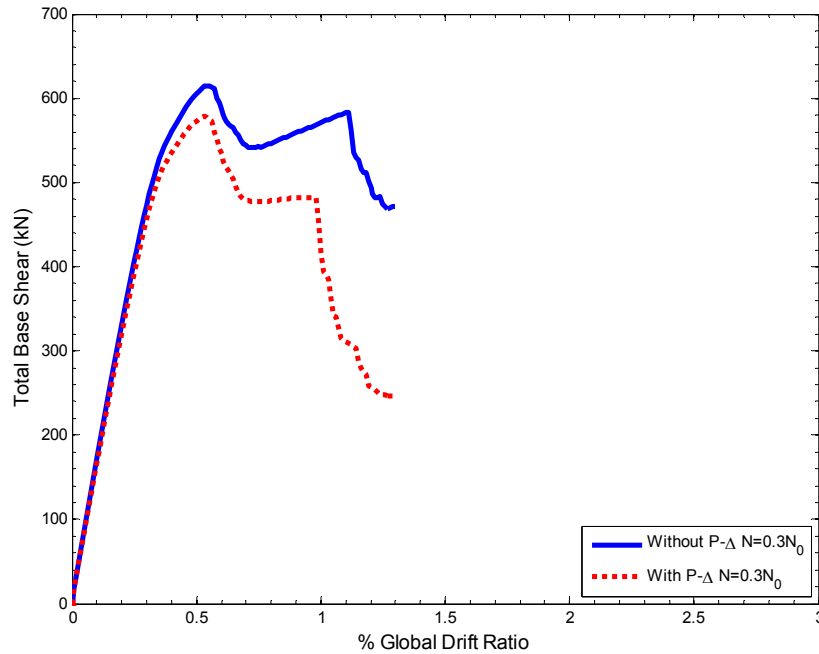


Figure 3.4 – Comparison of the Linear and Nonlinear Geometry in the Response of the Building without Wall ($N=0.3N_0$)

In Figures 3.2 to 3.4, as the axial force (N) increases from $0.1N_0$ to $0.2N_0$ and $0.3N_0$, the effect of nonlinear geometry on the structural frame without wall increases significantly. Thus the structural system loses ductility under nonlinear geometry as the axial force increases. The deformation limits are reduced since the column fails before it reaches its maximum deformation capacity under pure lateral stress, i.e. formation of the plastic hinges at the top of the first storey columns leads to a soft-storey in the structure.

Under $N = 0.3N_0$ in Figure 3.4, the system capacity is decreased by 20% at 1.3% drift ratio, resulting in practically a total loss of strength after this point.

3.2.1.1 Plastic Hinge Formation in the Structural Frame without Wall under Linear Geometry and $0.2N_0$ Axial Load

The order of the plastic hinge formations in the structural frame without wall is plotted in Figure 3.5. Plastic hinge formation starts with the right and left ends of the beams in the first and second floor, propagates to the bottom level of the columns in the first storey, and continues with the top end of the columns and each end of the beams in the upper stories. It is evident that the strong column – weak beam design has been satisfied in this hinge formation.

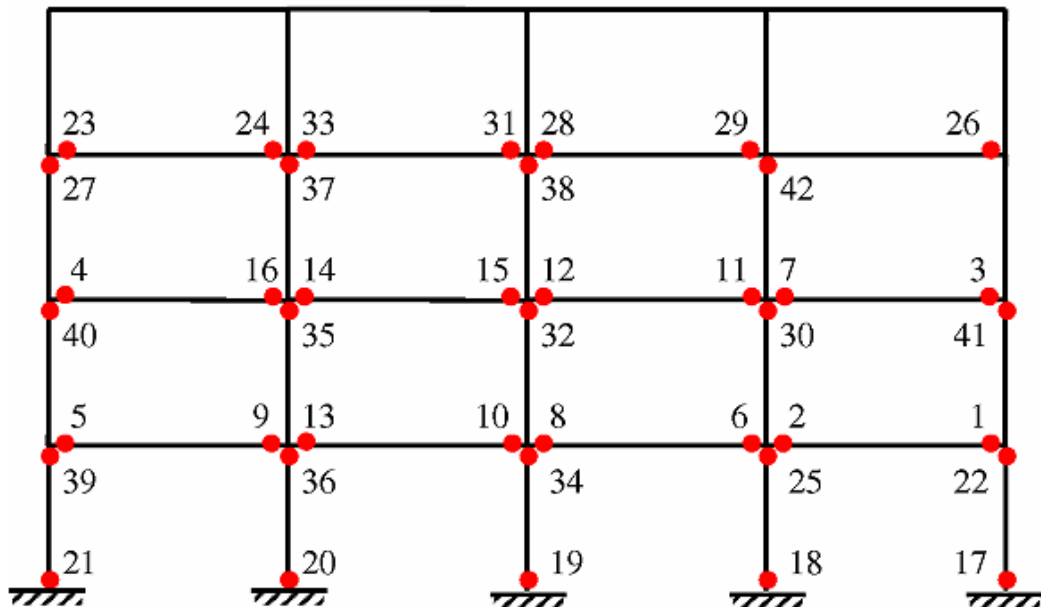


Figure 3.5 – Hinge Formations for Structural Frame without Wall under $0.2N_0$ Axial Load and Linear Geometry

The formation of the plastic hinges at the top end of the left two columns of first storey occur around 2% global drift ratio as seen in the load-displacement plot in Figure 3.6. The formation of these hinges actually

results in a soft storey mechanism, where the increase in the first storey drift ratio is evident from Figure 3.9.c presented later in this section.

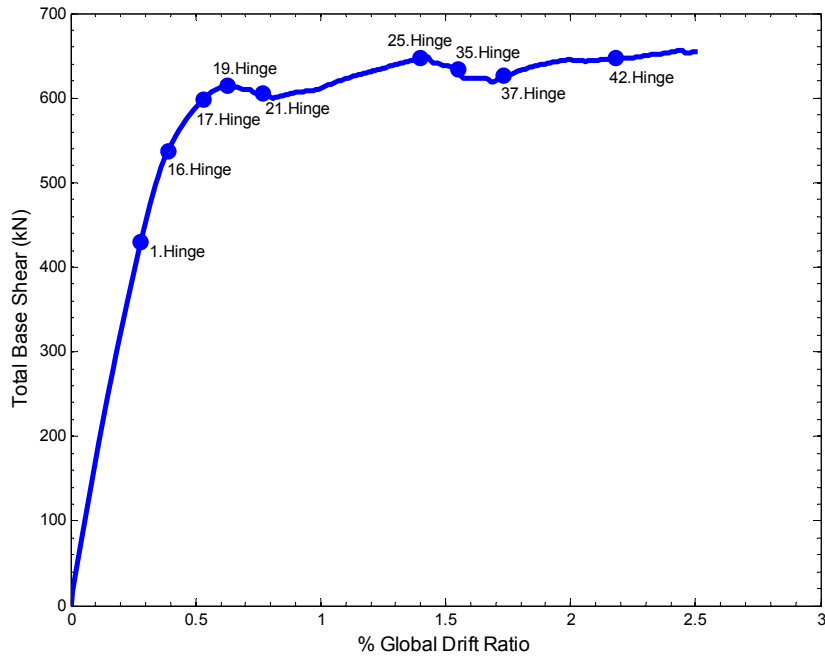


Figure 3.6 – Formation of Hinges on the Load-Displacement Plot of the Structural Frame without Wall under $0.2N_0$ Axial Load and Linear Geometry

The plots of bending moment versus curvature for the rightmost column at first storey and for the rightmost beam in the first floor of the structural frame are presented in Figures 3.7 and 3.8. While the beam shows a hardening behavior in Figure 3.8, the moment capacity at each end of the rightmost column at first storey shows significant strength deterioration due to the presence of axial load on it (even under linear geometry). It is important to emphasize that the present model for the columns does not consider buckling of the reinforcement, where this effect could be important especially when the columns present such a softening response as in Figure 3.7.

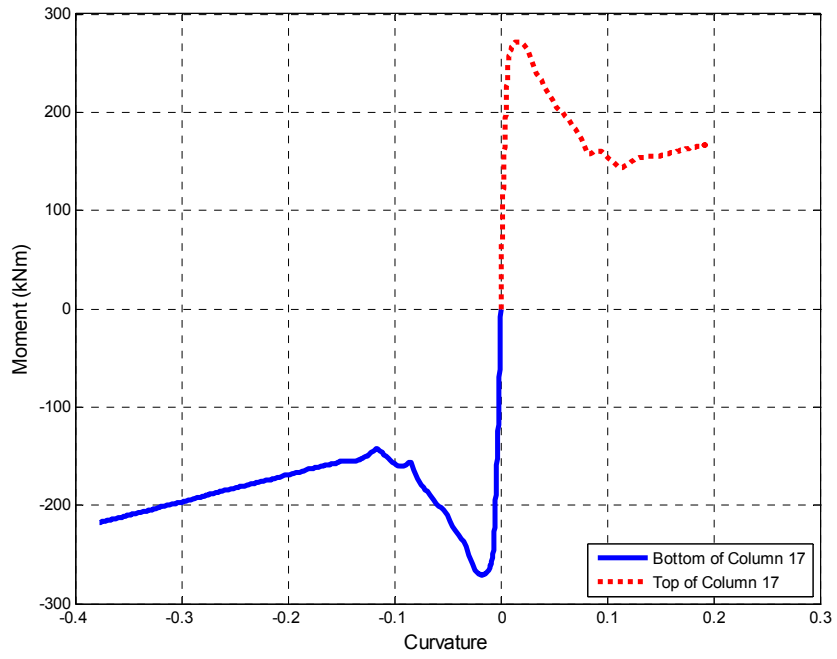


Figure 3.7 – Moment vs. Curvature Relation for the Rightmost Column at First Storey

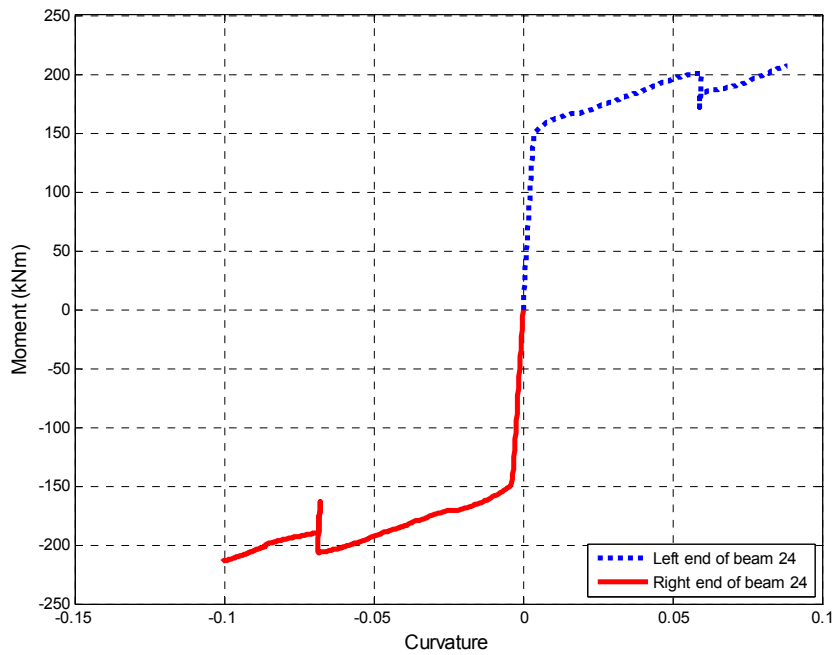


Figure 3.8 – Moment vs. Curvature Relation for the Rightmost Beam at First Floor

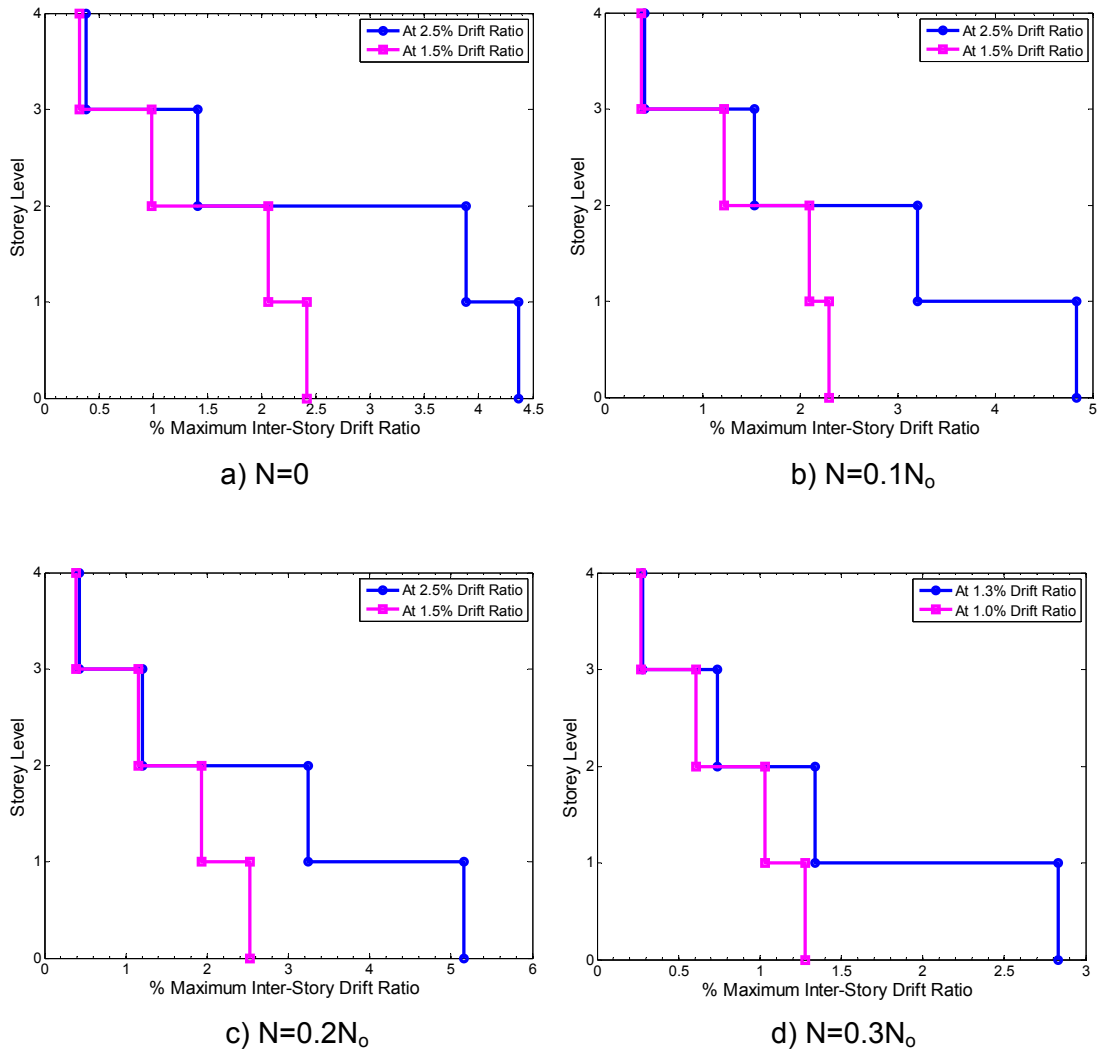


Figure 3.9 – Structural Frame without Wall under Linear Geometry

The maximum inter-story drift ratios for the structural frame without wall under linear geometry are presented in Figure 3.9. In Figure 3.9.a, the first and second storey drift ratios increase at the same rate for the unrealistic case of zero applied axial load. As the axial load increases from $0.1N_0$ to $0.3N_0$, the displacements are confined more and more to the first storey. When the structure reaches 2.5% global drift for the case of $0.2N_0$ in Figure 3.9.c, the first storey drift ratio exceeds 5% thus

practically resulting in a soft-storey mechanism. Under $0.3N_0$, the first storey drift ratio increases from 1.3% to 2.8% while the global drift merely increases from 1% to 1.3%. The doubling of the displacements at the first storey through such a small global drift explains the significant strength drop in the load-displacement plot in Figure 3.4.

3.2.1.2 Plastic Hinge Formation in the Structural Frame without Wall under Nonlinear Geometry and $0.2N_0$ Axial Load

The order of the plastic hinge formations in the structural frame with wall is plotted in Figure 3.10. Plastic hinges start forming first at the both ends of the beams in the first and second floor, then they propagate to the bottom end of the columns in the first storey, and continue with the top end of the columns and both ends of the beams in the upper stories

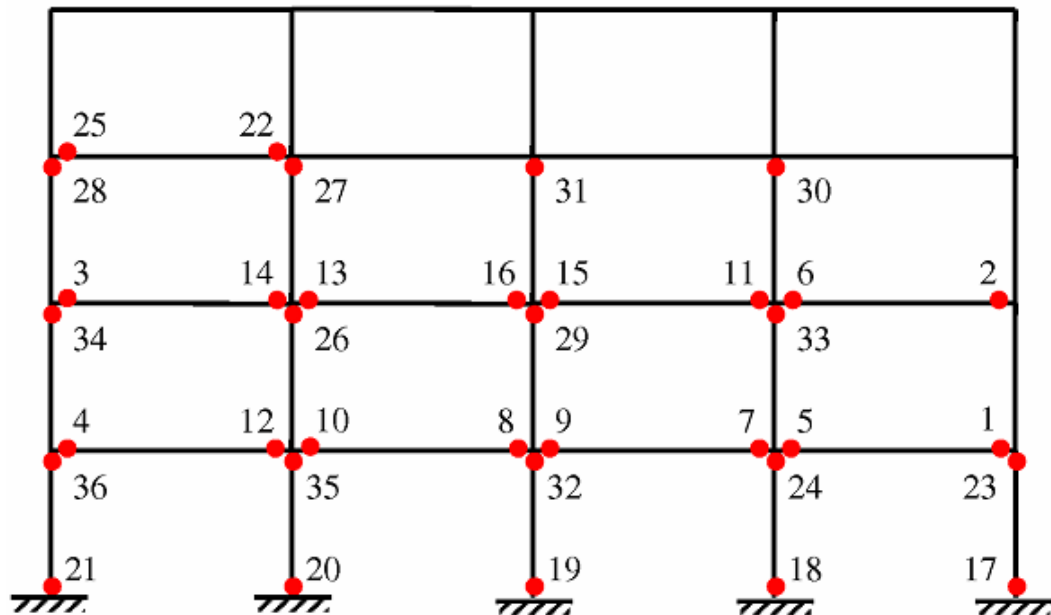


Figure 3.10 – Hinge Formations for Structural Frame without Wall under $0.2N_0$ Axial Load and Nonlinear Geometry

The plots of bending moment versus curvature for the rightmost column at first storey and for the rightmost beam in the first floor of the structural frame are presented in Figures 3.11 and 3.12. While the curvature demands for both ends of the column under nonlinear geometry are larger than the linear geometry case in Figures 3.7, this demand is reduced for the beam under nonlinear geometry when compared with its counterpart response under linear geometry in Figure 3.8.

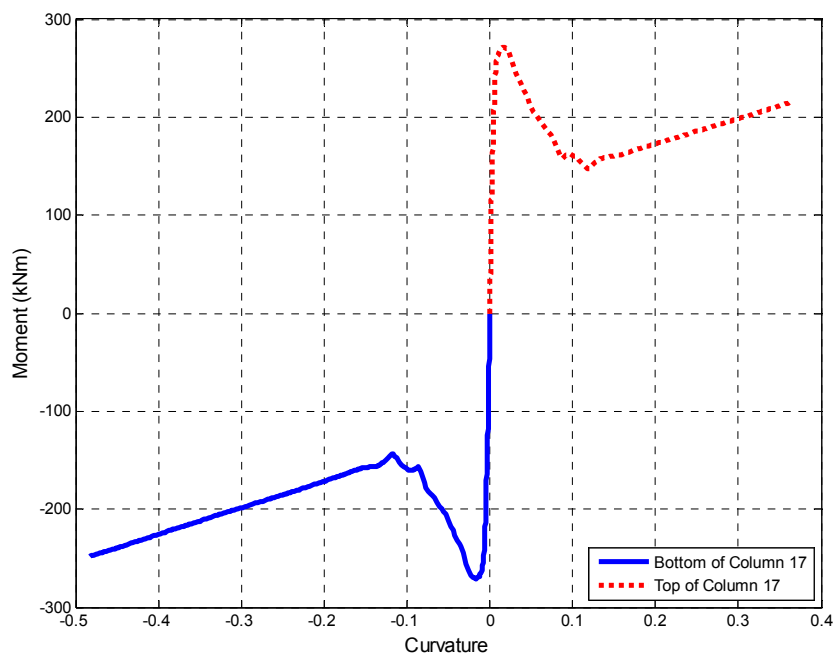


Figure 3.11 – Moment Curvature for Rightmost Column

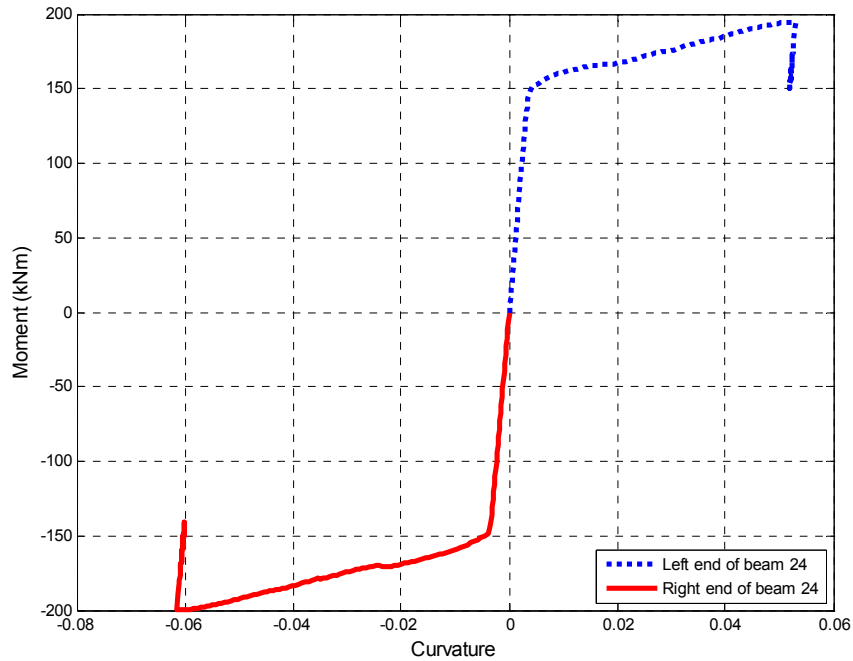


Figure 3.12 – Moment Curvature for Rightmost Beam

The maximum inter-story drift ratios for the structural frame without wall under nonlinear geometry are presented in Figure 3.13. The strength drop in the load-displacement plots under $0.2N_0$ and $0.3N_0$ in Figures 3.3 and 3.4 occurs due to the significant increase in the first storey drift ratios in Figure 3.13. While the response under $0.2N_0$ and linear geometry suggested a gradual spread of damage to the first and second stories in Figure 3.9.c, the displacements are localized to the first storey under nonlinear geometry at this axial load level in Figure 3.13.b, i.e. the first storey drift ratio jumps from 3% to 7% while the structure displaces from 1.5% to 2.5% global drift ratio. This is obviously an undesirable behavior for a structural system that is well-designed according to the strong column and weak beam design approach; thus special attention should be paid to the nonlinear geometric response of structures even under low levels of axial load.

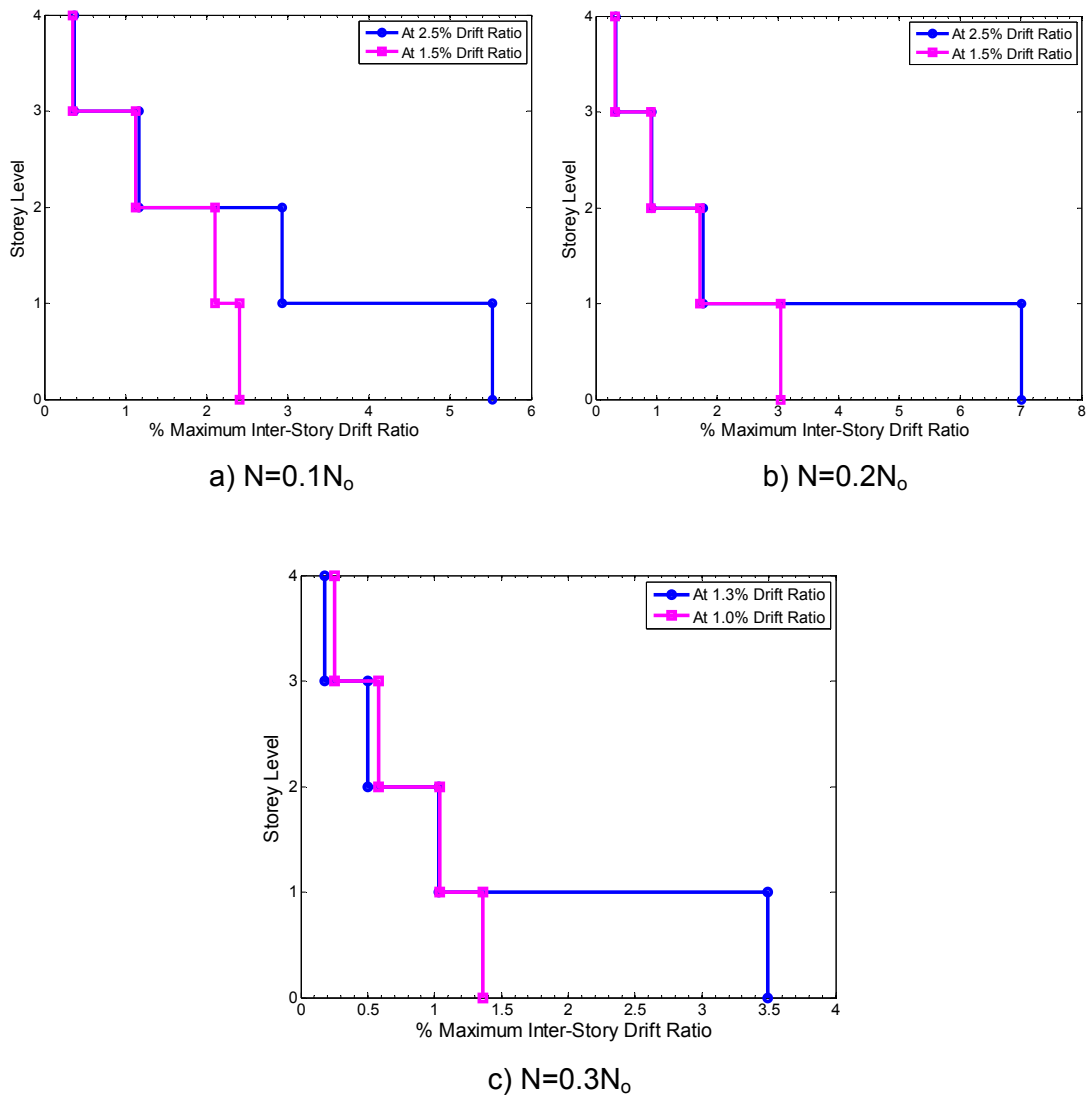


Figure 3.13 – Structural Frame without Wall under Nonlinear Geometry

3.2.2 Frame–Wall Structure

The walls, beams and columns of the frame–wall structure are modeled as described in Chapter 2, where the geometric and material properties were documented in detail.

A building structure subjected to a lateral force is shown in Figure 3.14, where the axial force applied at the top of each column is $0.25N$. As a result, the axial force at first story columns is equal to N under pure gravity loading. The axial force N is first taken as zero, and then it is changed with respect to the axial load carrying capacity of the columns calculated in Equation (3).

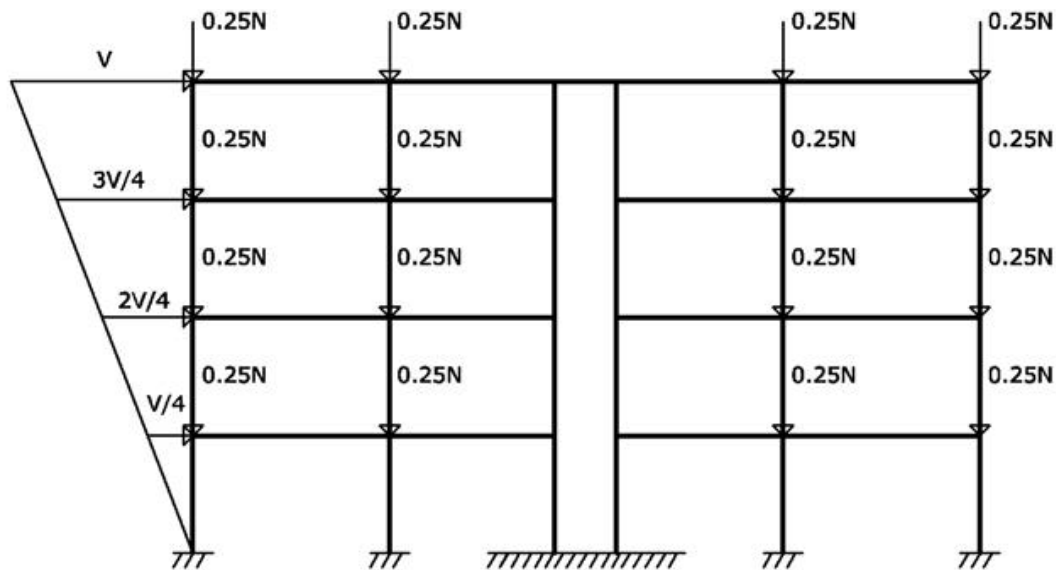


Figure 3.14 – Profile of Lateral Force Applied to the Building Structure

3.2.2.1 Effect of Nonlinearity in the Wall

Load-displacement curves of the building without wall, and with elastic and inelastic walls are presented in Figure 3.15. All the beams, columns and the case of inelastic walls are modeled with the nonlinear beam-column elements described in Chapter 2. The length of both the elastic and inelastic walls is taken as 140cm in this comparison.

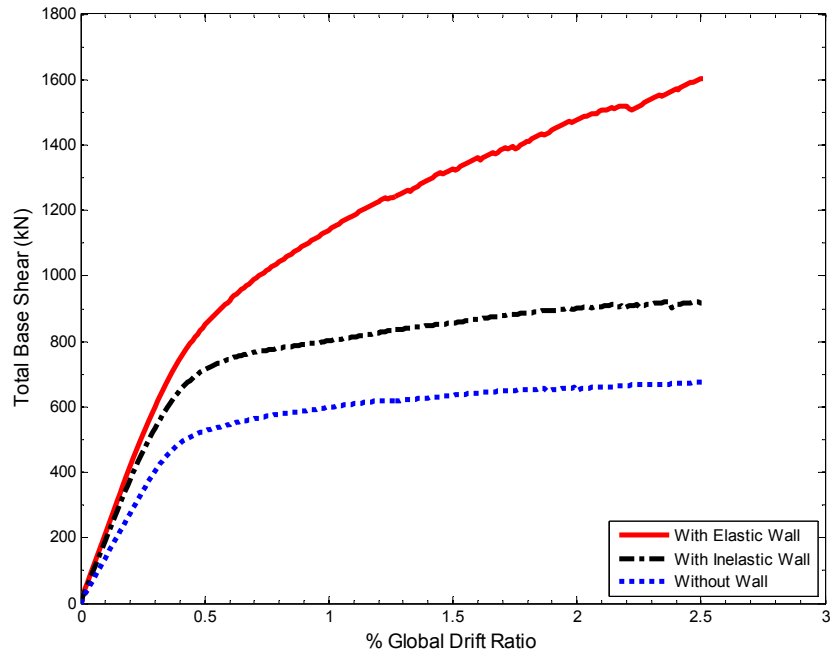


Figure 3.15 – Comparison of the Load-Displacement Responses of the Building without Wall and with Elastic and Inelastic Walls under Zero Axial Force

The stiffness and load carrying capacity of the building without wall is much less than those of the building with walls. The inelastic wall model is able to simulate flexure yielding, thus this reduces the lateral load carrying capacity of the structure when compared with the elastic wall model. The importance of using material nonlinearity in wall analysis is evident from this comparison.

3.2.2.2 Influence of Axial Force in the Frame-Wall Structural System

The building with inelastic shear wall is investigated under varying levels of axial force applied on the columns as shown in Figure 3.14. The length of the walls is taken as 140 cm in this analysis.

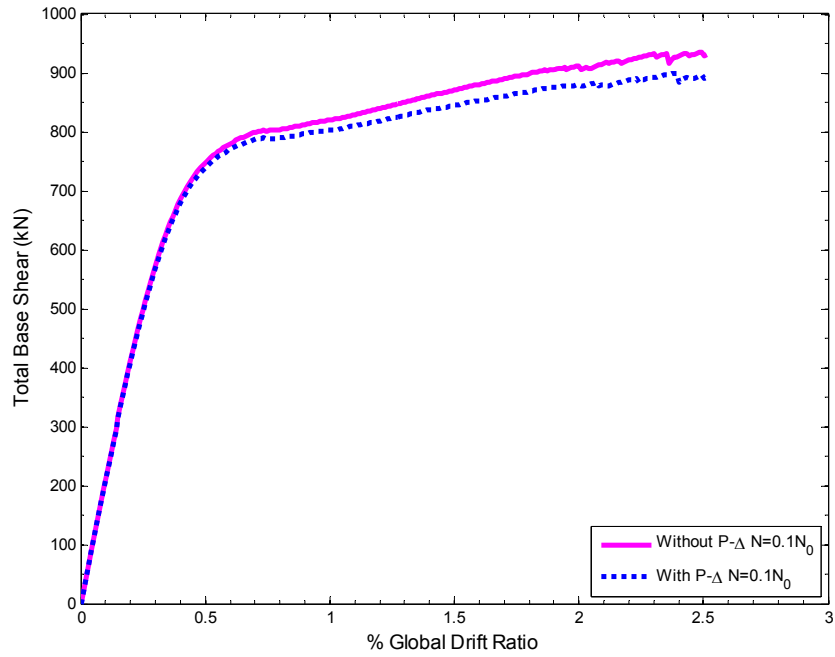


Figure 3.16 – Comparison of the Linear and Nonlinear Geometry in the Response of the Frame–Wall ($N=0.1N_0$)

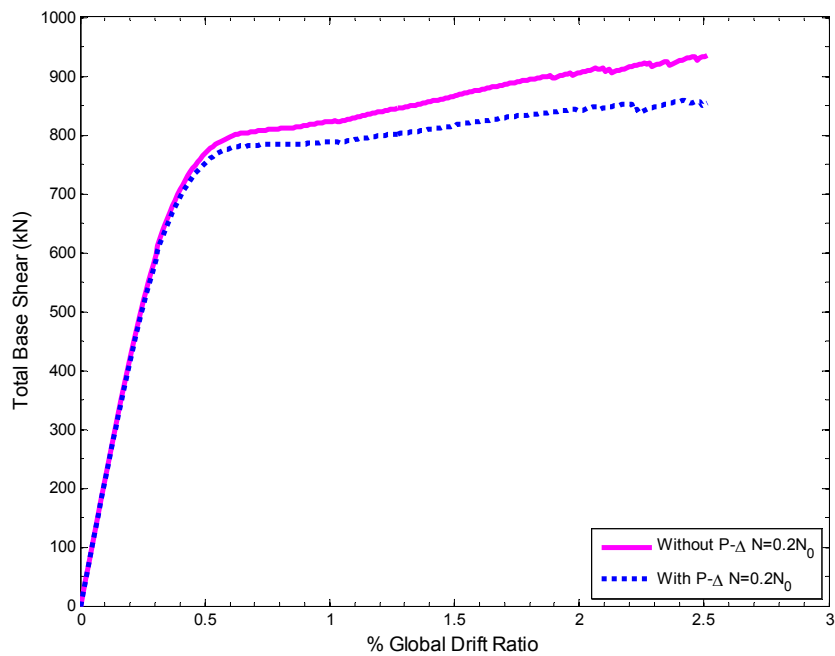


Figure 3.17 – Comparison of the Linear and Nonlinear Geometry in the Response of the Frame–Wall ($N=0.2N_0$)

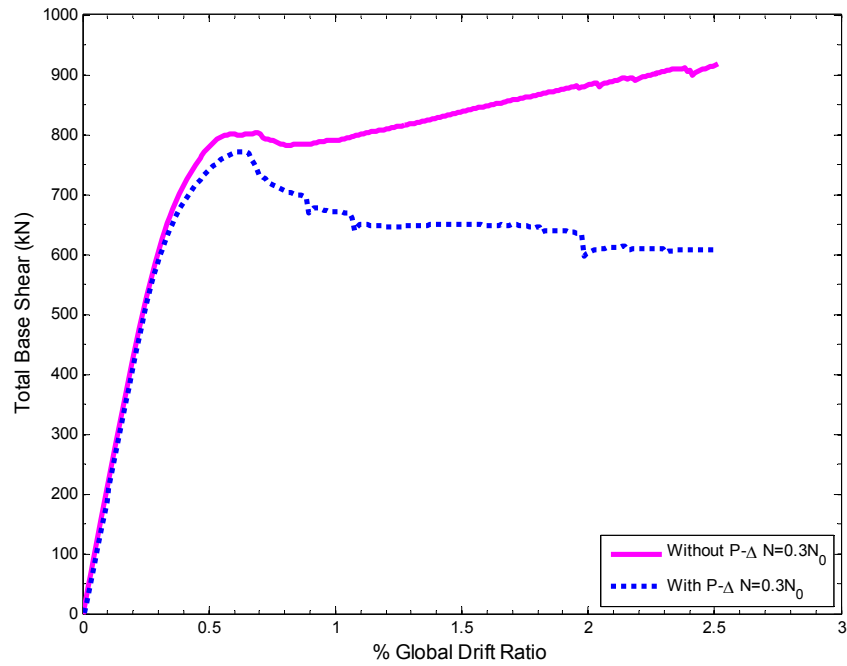


Figure 3.18 – Comparison of the Linear and Nonlinear Geometry in the Response of the Frame–Wall ($N=0.3N_0$)

In general, nonlinear geometric effects are less pronounced in the frame-wall system than the frame without wall system for the same levels of applied axial forces. In Figures 3.16 and 3.17, nonlinear geometric effect on the load-deformation response of the frame–wall structure is negligible under low levels of applied axial force. On the other hand, nonlinear geometric effect on the frame-wall system under $0.3N_0$ axial load is clearly seen in Figure 3.18. Thus we conclude that moderate levels of applied axial force in the columns of a frame-wall system can result in a loss of load carrying capacity of the structure when nonlinear geometric effects are considered in the analysis.

Table 3.1 – Comparison of the Results of the Frame–Wall System with Different Wall Lengths

Maximum Lateral Load Capacity of FW L=140 cm			
Axial Load Level	w/o P-Δ (kN)	w P-Δ (kN)	% Change
0.1N _o	940	900	4.25
0.2N _o	930	855	8.06
0.3N _o	915	773	15.52
Maximum Lateral Load Capacity of FW L=200 cm			
Axial Load Level	w/o P-Δ (kN)	w P-Δ (kN)	% Change
0.1N _o	1080	1044	3.33
0.2N _o	1075	1006	6.42
0.3N _o	1053	948	9.97
Maximum Lateral Load Capacity of FW L=250 cm			
Axial Load Level	w/o P-Δ (kN)	w P-Δ (kN)	% Change
0.1N _o	1218	1185	2.71
0.2N _o	1213	1152	5.03
0.3N _o	1183	1110	7.02

In Table 3.1, we present numerical results from the analysis of the frame-wall system with wall lengths of 140 cm, 200 cm and 250 cm. The effect of nonlinear geometry on the frame–wall structure is low under 0.1N_o and 0.2N_o applied axial loads, while the situation changes under 0.3N_o. As the length of wall increases, the influence of nonlinear geometry on the frame-wall system is reduced. It is observed that the influence of axial force with or without the consideration of nonlinear geometry reduces significantly for the wall with 250 cm length. These results suggest that an optimum wall length should be used in the retrofit of buildings with walls or in the design of frame-wall type systems in order to eliminate the possibility of loss of strength in the post-yield branch under nonlinear

geometry. More importantly, a nonlinear analysis as performed in this thesis should validate the ductility of the load-displacement curve.

3.2.2.3 Bending Moment Diagram and Curvature Distribution in the Walls of the Frame-Wall System

The bending moment diagram and the curvature distribution along the walls of the frame-wall system for 140 cm and 250 cm wall length are presented in Figures 3.19 and 3.20.

In the bending moment diagrams, the moment jumps at each floor level occur due to the moment carried in the joining beams. A centerline moment value is picked at each floor level, and an average bending moment diagram for the walls is plotted.

Since the 250 cm wall carries a larger proportion of the lateral load, the bending moment at the base of the wall increases significantly when compared with the results of the 140 cm wall length. On the other hand, the comparison of the moments at the top reveals a much different story: the moment at the top level for the 250 cm wall length reduces to $1/8$ of the base value, while this ratio is around $1/3$ for the 140 cm wall length. Thus, the distribution of moment in the walls is more uniform in frame-wall structures with lower wall lengths.

The inflection point in the average moment diagram occurs in the middle of the second storey for the 140 cm wall length, and the same point is observed to lie in the middle of third storey for the 250 cm wall length.

In general we observe that up to 95% of the response along the wall height practically remains in the elastic range from the curvature

distribution plots in Figures 3.19 and 3.20. The curvature demand at the base of the wall is halved as a result of the increase in the wall thickness from 140 cm to 250 cm. Nonlinearity in the 140 cm wall is confined to the base point, and there is little nonlinear action at the next integration point above the base point for this wall. On the other hand, there is visible nonlinear action at the base point and the next integration point above the base point in the 250 cm wall.

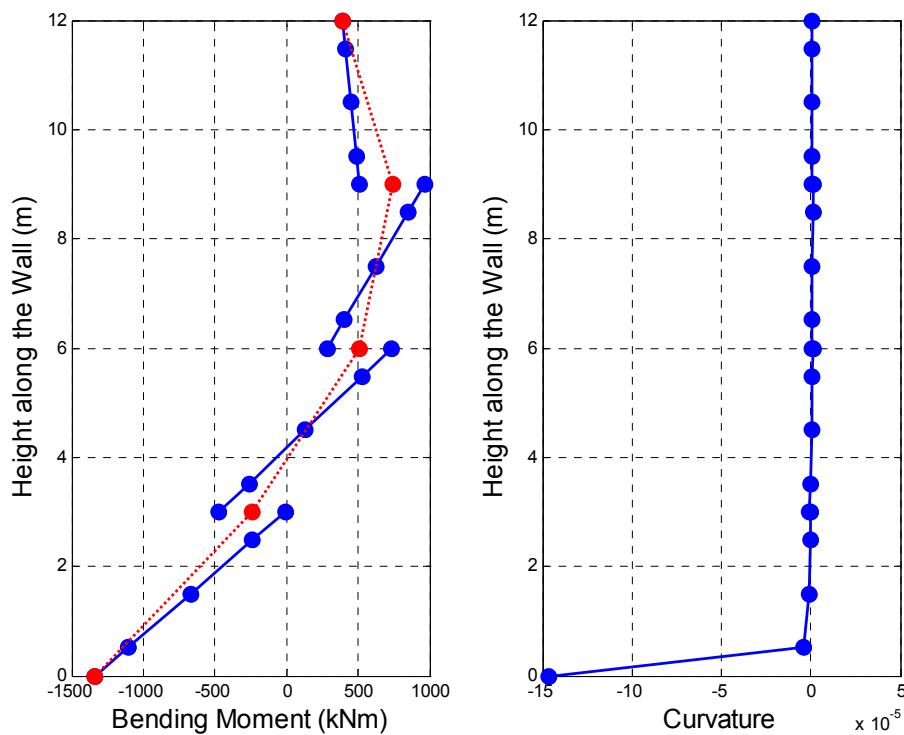


Figure 3.19 – Frame-Wall System with 140cm Wall Length

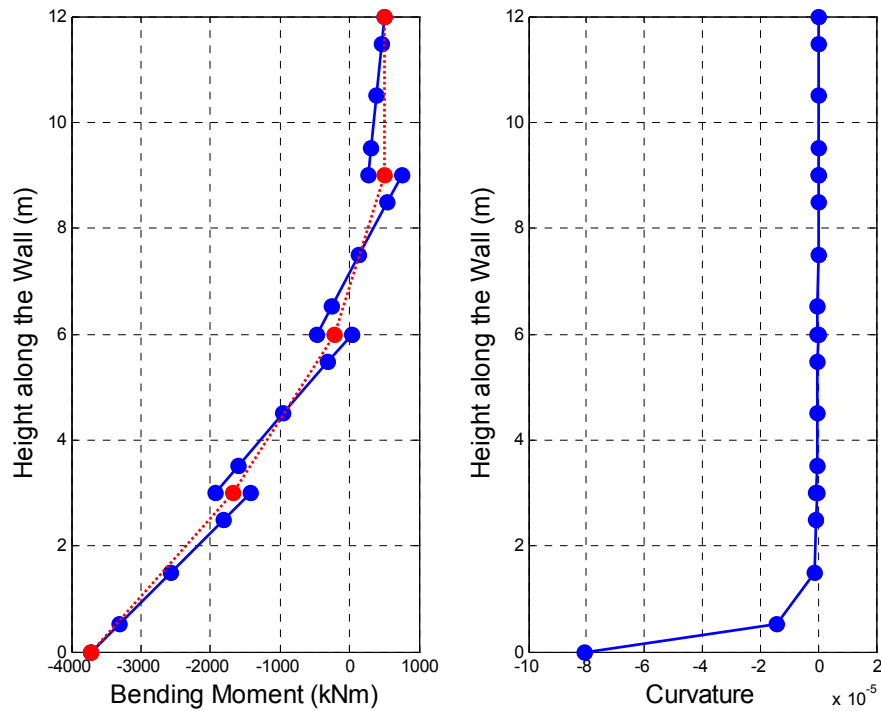


Figure 3.20 – Frame-Wall System with 250cm Wall Length

3.2.2.4 Load Redistribution due to Yielding in the Walls

The influence of wall stiffness in the load redistribution between the walls and columns of the frame-wall system is studied in this section. Wall lengths of 140 cm, 200 cm, and 250 cm are selected for comparison, and only linear geometric analysis under zero applied axial force is considered. All the members of the frame-wall structure are modeled as described in Chapter 2, where geometric and material properties are presented in detail.

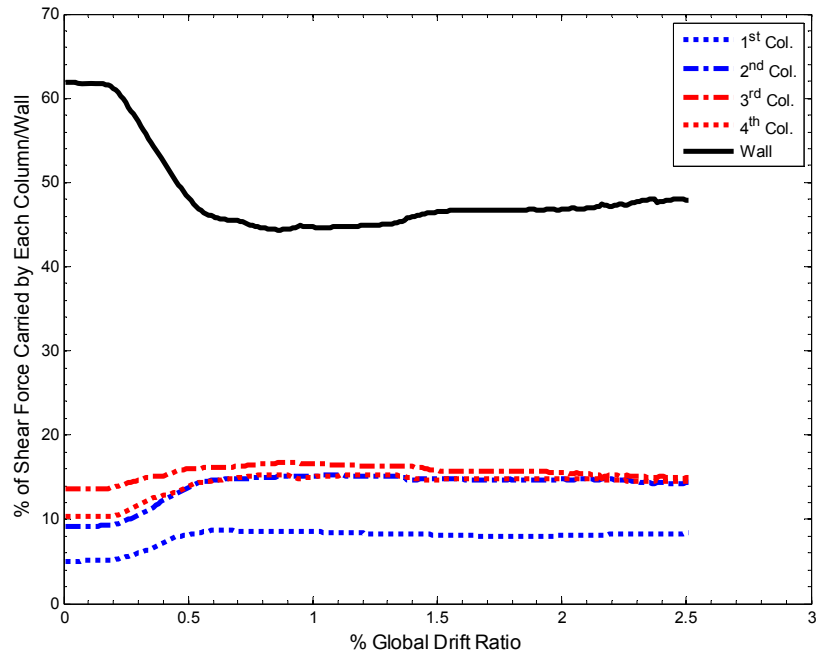


Figure 3.21 – Percentage of Shear Force Carried by Each Column/Wall (Wall Length=140 cm)

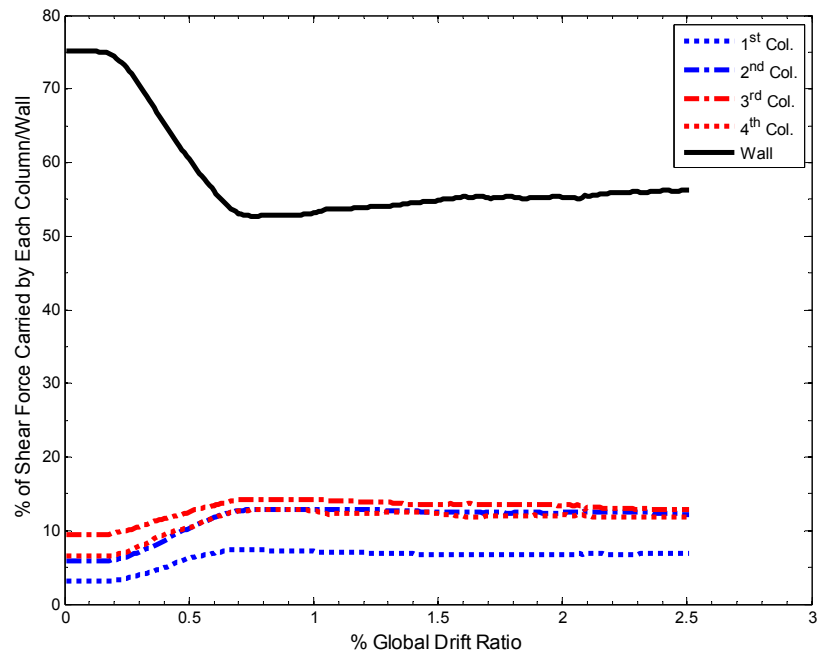


Figure 3.22 – Percentage of Shear Force Carried by Each Column/Wall (Wall Length=200 cm)

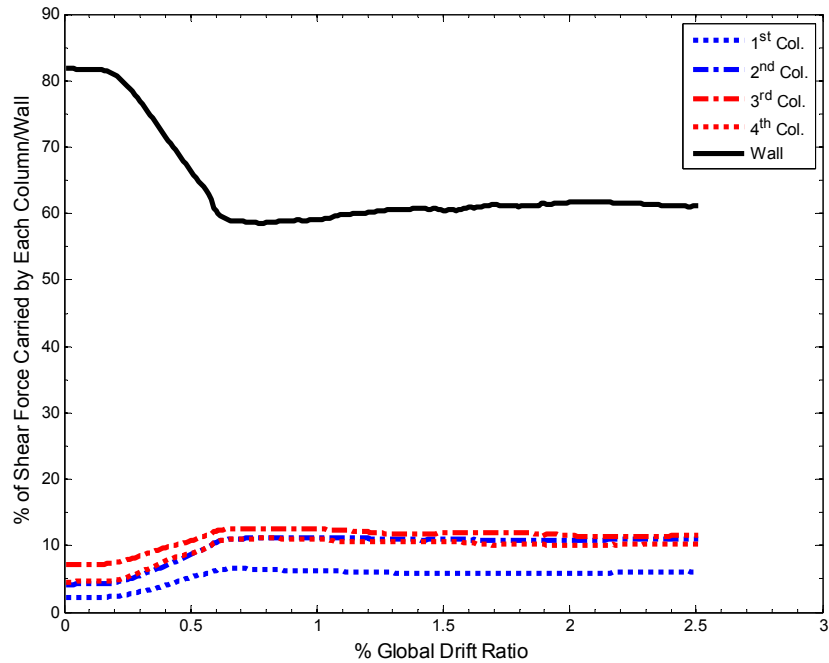


Figure 3.23 – Percentage of Shear Force Carried by Each Column/Wall (Wall Length=250 cm)

In Figures 3.21 to 3.23, as the wall length (stiffness) increases, the percentage of lateral force carried by the walls increases naturally. Once the wall yields, the percentage of lateral force carried by walls drops by almost 30%, and the load is redistributed to the columns. As a result, the columns should be strong enough to meet this demand. The load redistribution starts at around 0.25% global drift ratio in the considered buildings.

The frame–wall system considered in this thesis is loaded from left (Figure 3.14). For the unrealistic case of zero applied axial force on the columns, the two columns on the left and right of the wall are under tension and compression, respectively. The reason of this load distribution is the combined effect of the geometry of the structure and

the loading direction with respect to shear wall located at the axis of symmetry. The tensile axial force in the leftmost column reaches to 8.54% of the absolute value of its maximum compressive load carrying capacity (N_0) in Equation 3. The axial force on the left column closer to the wall does not even reach to a countable percent of its capacity. The columns on the right side of the shear wall are under compression. The rightmost column carries a compressive axial force of almost 9.1% of the maximum compressive load carrying capacity (N_0), and the level of compressive axial force in the right column next to the shear wall doesn't reach to a countable percent. The magnitude of the axial forces on the outermost columns on both sides is not exactly the same despite the fact that the structure is symmetric about the wall. This discrepancy stems from the difference of the concrete's response under tensile and compressive forces. Furthermore, there isn't any considerable axial force on the shear wall.

The finite element models used in this study can capture axial force-bending moment interaction through the use of fiber discretization of the section. Thus, the differences in the load carrying capacities in the tension and compression zone are explained through this interaction phenomenon.

Finally, we would like to present the load-displacement responses of the walls with different wall lengths in Figure 3.24. Both the stiffness and lateral load carrying resistance of the frame-wall structure increases as the wall length increases.

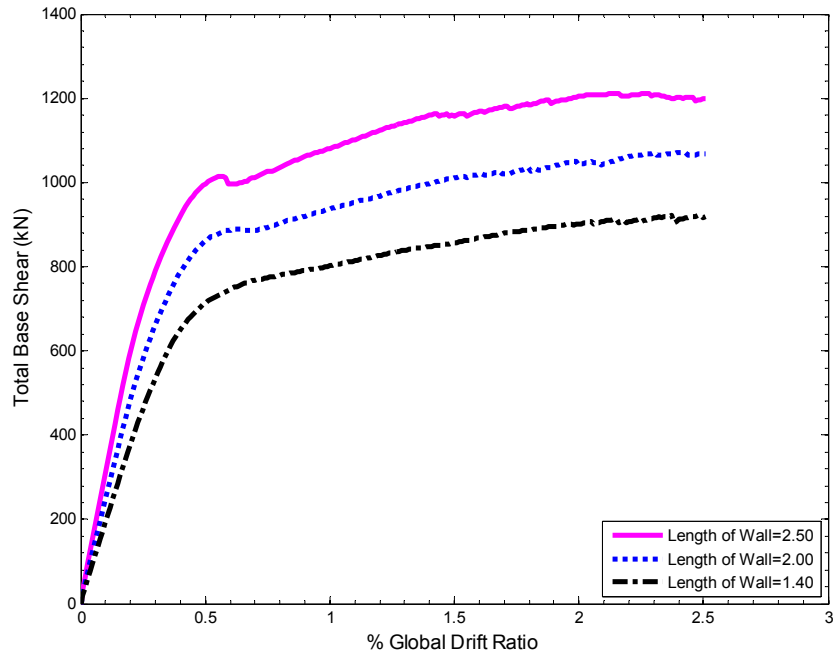


Figure 3.24 – Response of Frame-Walls with Different Wall Lengths under Zero Axial Force

3.3 NONLINEAR DYNAMIC ANALYSIS

In this section, the performance of the structural frame without wall and the structural frame with both elastic and inelastic shear walls having 140 cm lengths are investigated under several ground motion data. The results of the time history analyses of the three building structures (frame without wall, frame-wall with elastic and inelastic walls) are presented in the following.

In the analyses, all structural elements (columns, beams and walls) are assumed to have their own masses. These masses are calculated and distributed to each node. Half of the total mass of each column and beam joining at a node is assigned to the nodal mass. The dead weight of the

slab for a clear span of 5 m and thickness of 12 cm as described in Section 2.3.2 is also taken into account in the nodal masses. Furthermore, the mass density of concrete is taken as 2400 kg/m^3 in the analyses. The acceleration values in the original record, in terms of g (gravitational acceleration), are converted to meters per second by multiplying by 9.81. A damping ratio of 5% is used in the analyses.

The effects of earthquakes on the structures vary with the soil conditions, focal depth of the ground motion, duration of the shaking, etc. For example, the 1957 Mexican Earthquake caused extensive damage to the multistory buildings in Mexico City but not to the small buildings. The earthquake was located 170 to 200 miles from Mexico City. The reasons for the pocket of damage in Mexico City are attributable to the poor ground conditions that did not damage the weak but short-period structures (Steinbrugge and Bush 1960). In this study, the above mentioned parameters were not investigated; the whole purpose is to observe the effects of different levels of earthquake intensity on a structure.

The characteristic of earthquake records which is applied directly to the base of the building structures in this thesis are shown in Table 3.2. The ground motion data for these are downloaded from PEER Strong Ground Motion Database on the internet.

Table 3.2 – The Characteristic of Earthquake Records

Earthquake Records	Component	PGA (g)	Duration considered
Chi-Chi, Taiwan	CHY080-W	0.968	100s
Coalinga, California	D-CHP090	0.605	45s
Erzincan, Turkey	ERZ-NS	0.515	30s

Time history analyses are performed on the three building models and the following parameters are compared: 1) Total base shear versus drift ratio of the top storey for the three models; 2) The magnitude of the shear force at the base of the shear walls with lengths 140 cm, 200 cm and 250 cm for the frame-wall model with inelastic walls.

3.3.1 Total Base Shear versus Drift Ratio of the Top Storey

The base shear history graphs obtained from time history analysis for the three sample building structures are presented in Figures 3.25 to 3.27 under the earthquake records in Table 3.2.

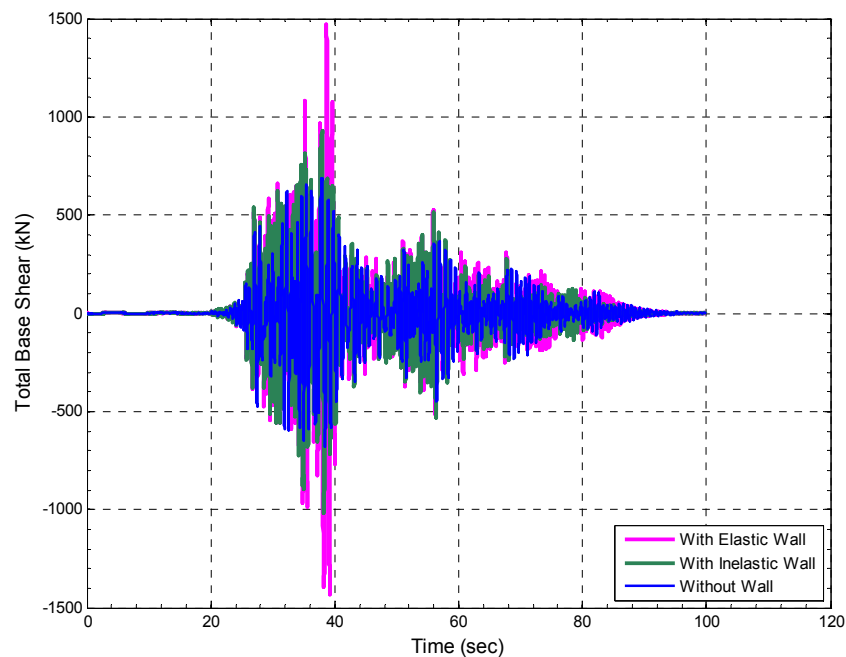


Figure 3.25 – Total Base Shear vs. Time History for Chi-Chi Earthquake Record

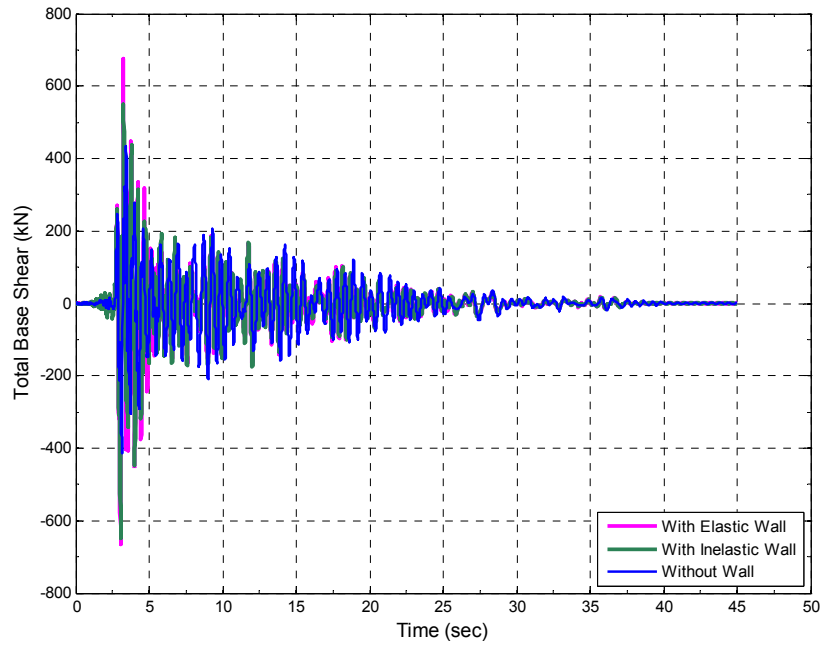


Figure 3.26 – Total Base Shear vs. Time History for Coalinga Earthquake Record

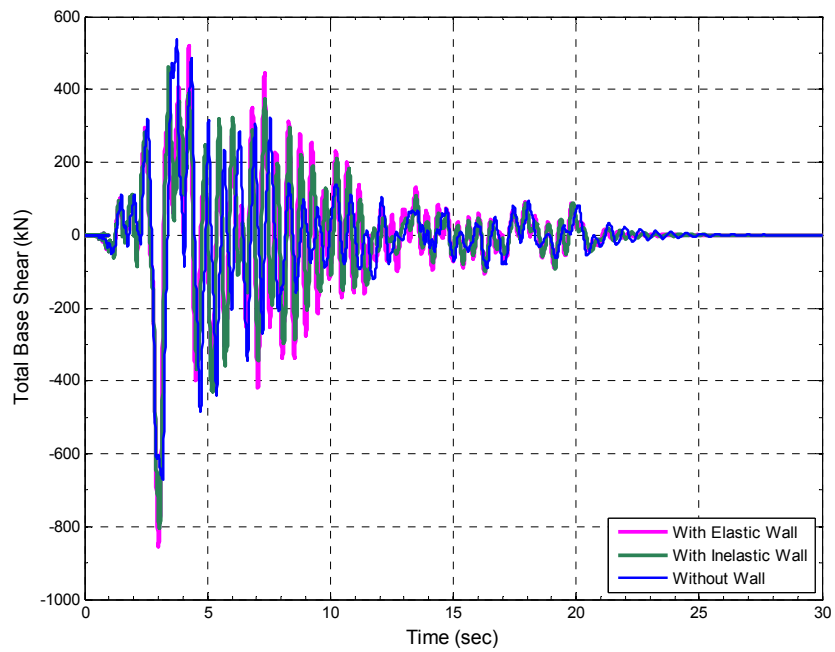


Figure 3.27 – Total Base Shear vs. Time History for Erzincan Earthquake Record

In Figures 3.25 to 3.27, the structural system having elastic wall clearly takes more shear at the basement level than the others in all of the ground motion data. For more in depth analyses of the results, we draw the percentage global drift ratio versus time history plots for the three building models in Figures 3.28 to 3.30 for the same ground motions.

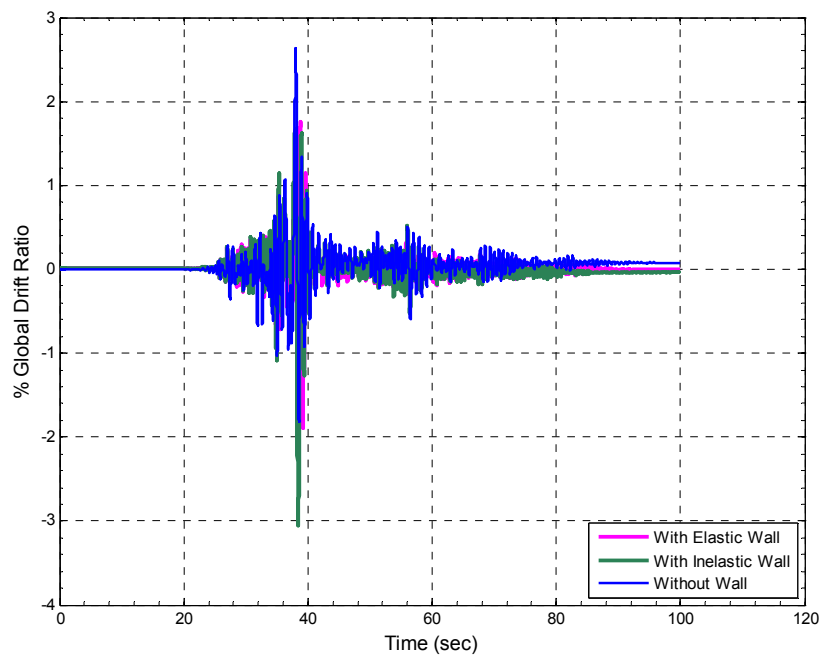


Figure 3.28 – Global Drift Ratio vs Time History for Chi-Chi Earthquake Record

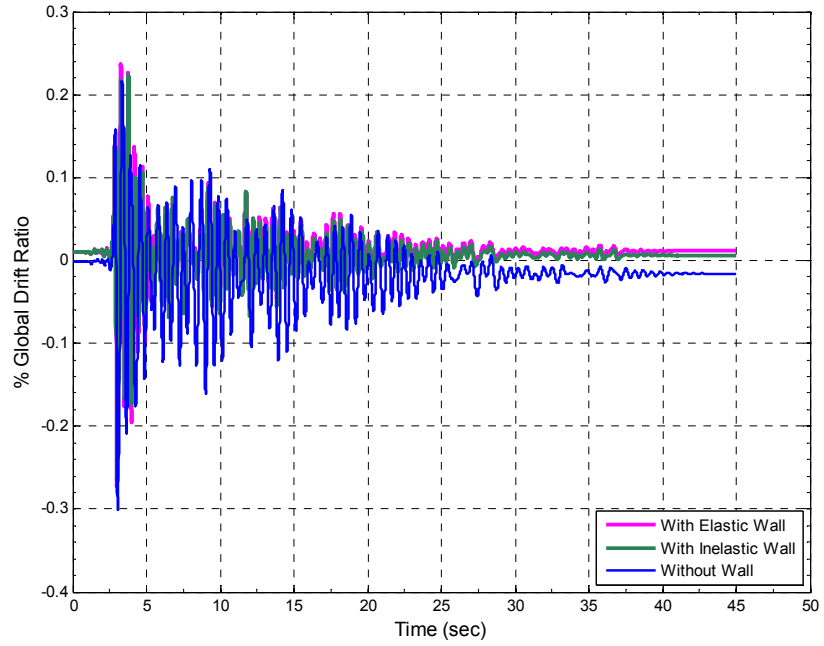


Figure 3.29 – Global Drift Ratio vs Time History for Coalinga Earthquake Record

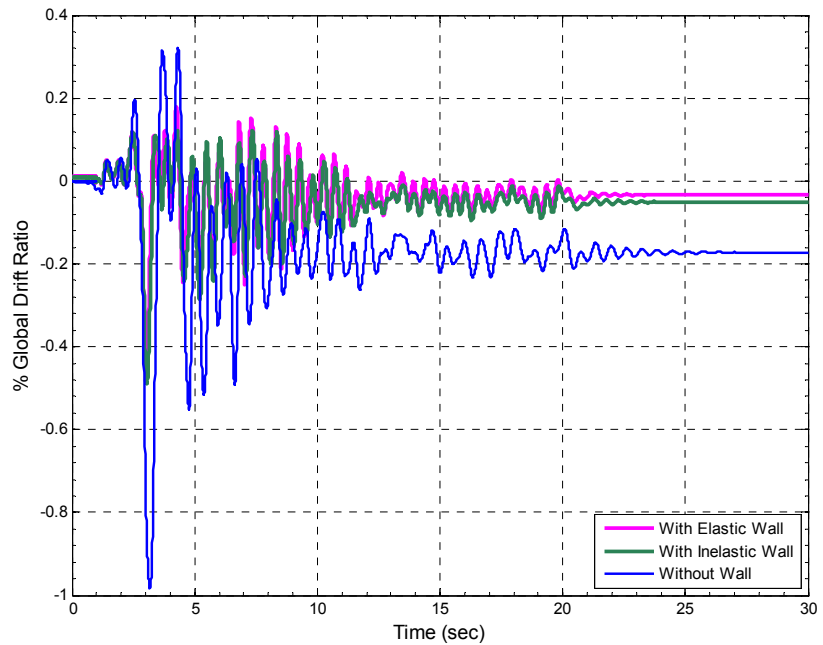


Figure 3.30 – Global Drift Ratio vs Time History for Erzincan Earthquake Record

As we can see in Figure 3.30, the global drift ratio is largest when there is no wall. Since the stiffness of the wall enhances the resistance to the lateral drift; it is naturally expected from the system to be more rigid laterally under moderate levels of ground motion. On the other hand, in Figure 3.28, frame-wall system with inelastic wall goes through a slightly larger global drift than the frame without wall system under strong ground motion. Despite increased drift ratios in the frame-wall system, the level of permanent damages are less than that observed in the frame without wall.

The permanent damage due to Coalinga Earthquake is almost non-existing in Figure 3.29, suggesting the fact that these buildings remained mostly in the elastic range of response, and dissipated earthquake energy mostly through viscous damping.

If we look closer to the response from Erzincan earthquake record in Figure 3.30, the biggest permanent damage occurs in the frame without wall. The permanent damages are below 0.2%, and appear in all of the three models of the building approximately after 12 seconds.

Although Erzincan Earthquake has the smallest duration in Table 3.2, the permanent damage occurred due to this earthquake is similar in magnitude to the that observed due to Chi-Chi Earthquake and larger than Coalinga Earthquake record.

These results show us the complexity of the nonlinear time history analyses. The selection of a frame-wall structure may not always be advantageous in resisting earthquakes, i.e. the characteristics of the site and the structure should be evaluated in depth for a final decision on the selection of the suitable structural system to resist strong motions. This thesis did not focus on these topics.

3.3.2 Influence of Wall Stiffness

In this part, the influence of wall stiffness on the total base shear force and the percentage global drift ratio of the frame-wall structure are studied under the earthquake records given in Table 3.2. The results of the total base shear force for the 140 cm, 200 cm and 250 cm wall lengths of the frame-wall structure are compared for the three ground motion data in Figures 3.31 to 3.33.

The maximum base shear forces occur in Chi-Chi Earthquake, since it has the biggest PGA among the three. For the results obtained from Chi-Chi Earthquake in Figure 3.31, the frame-walls with length 250cm attains maximum base shear forces and a similar trend is also seen for Erzincan Earthquake in Figure 3.33. For Coalinga Earthquake in Figure 3.32, the frame-walls with lengths 200 cm and 250 cm attain maximum base shear forces that are both larger than the response obtained from 140 cm case. From these figures, we conclude that changing the wall stiffness has a small effect in changing the total base shear force resisted by a frame-wall system during an earthquake. The real difference will actually be seen in the seismic distortion levels.

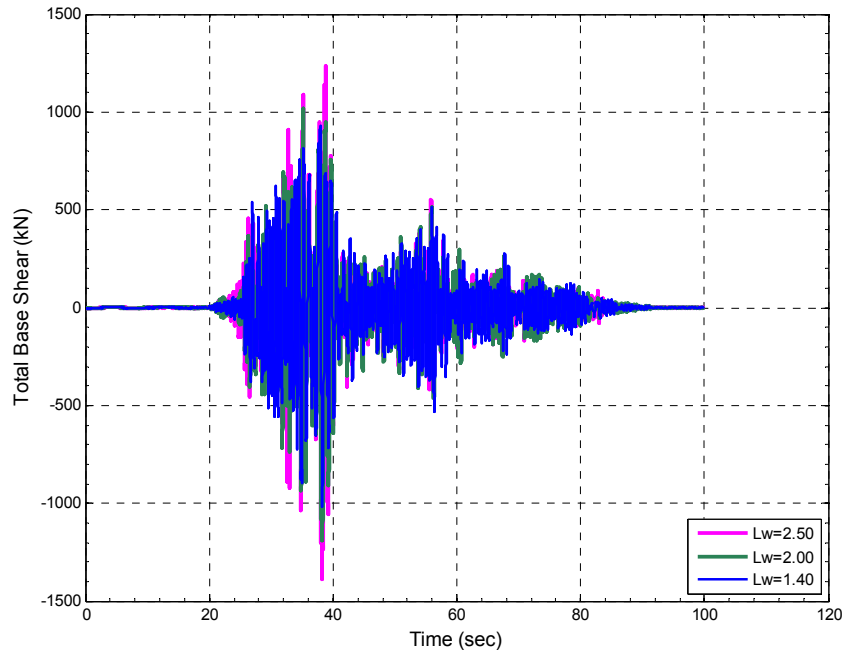


Figure 3.31 – Base Shear Force vs. Time History for Chi-Chi Earthquake Record

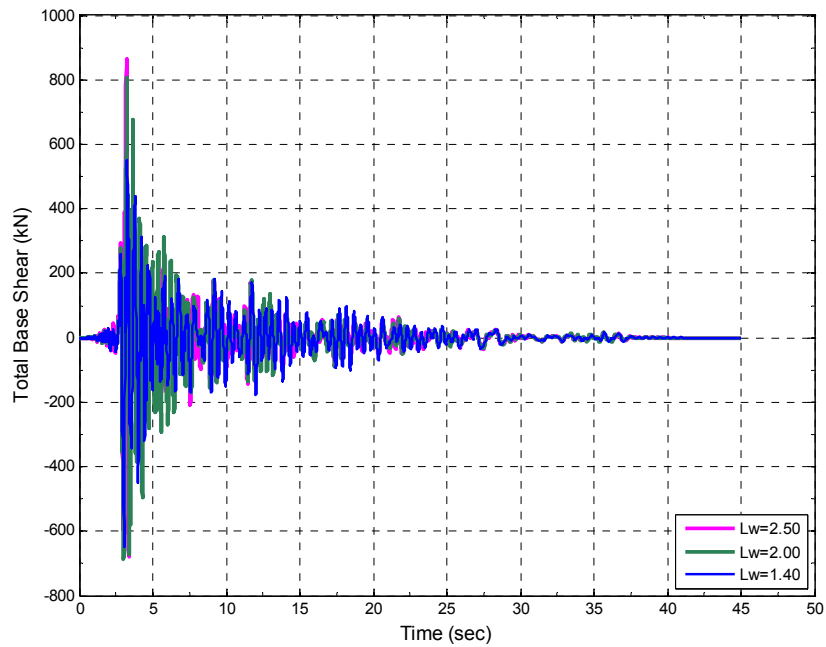


Figure 3.32 – Base Shear Force vs. Time History for Coalinga Earthquake Record

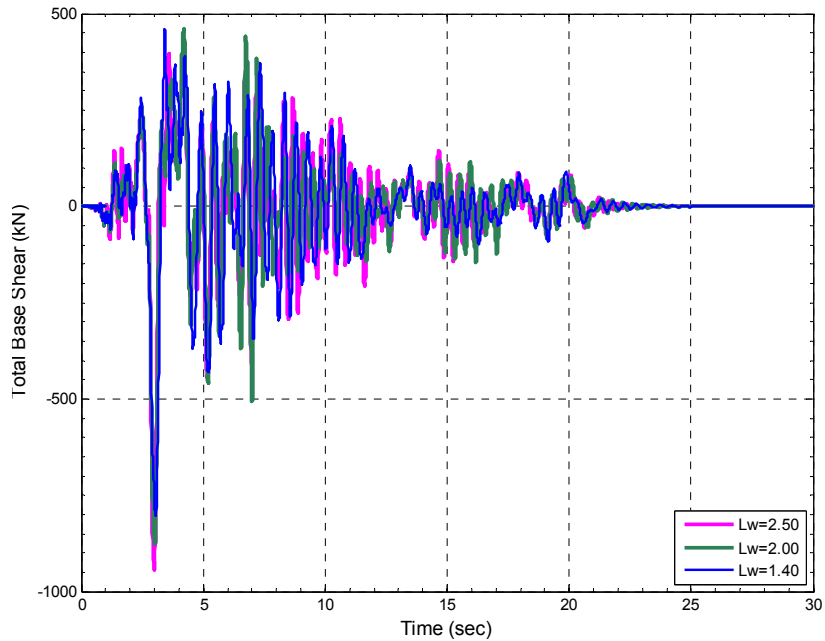


Figure 3.33 – Base Shear Force vs. Time History for Erzincan Earthquake Record

In Figures 3.34 to 3.36, the drift ratio is largest with the 140 cm wall system due to its flexibility. For Erzincan Earthquake in Figure 3.36, all the frame-wall structures enter into plastic region and continue to vibrate around a permanent deformed position approximately after 12 seconds. For Chi-Chi Earthquake in Figure 3.34, the 250cm wall system enters into plastic region and continues to vibrate around a slight permanent deformed position approximately after 40 seconds, while the other wall systems vibrate basically in the elastic region. This results show that design of wall length in the structural system is very important. Although the frame-walls with length 250 cm attain maximum base shear forces that are both larger than the response obtained from 140 cm case, permanent damage with 250cm case is larger than 140 cm case. For Coalinga Earthquake in Figure 3.35, all the wall systems vibrate basically in the elastic region.

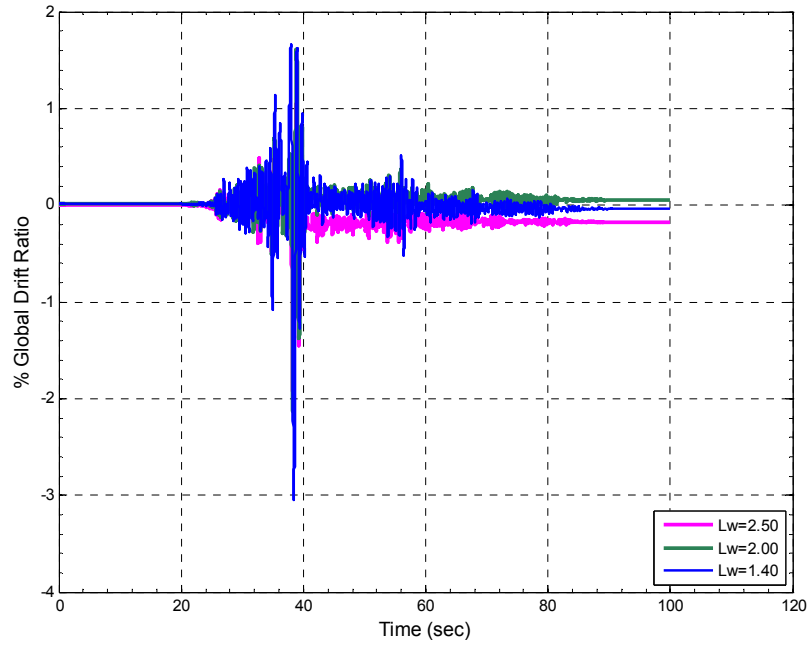


Figure 3.34 – Global Drift Ratio vs. Time History for Chi-Chi Earthquake Record

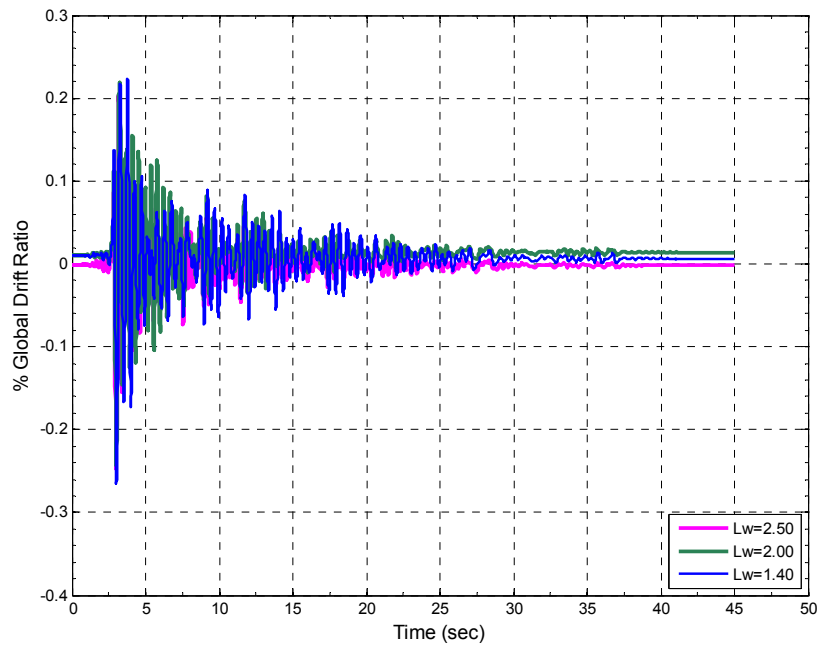


Figure 3.35 – Global Drift Ratio vs. Time History for Coalinga Earthquake Record

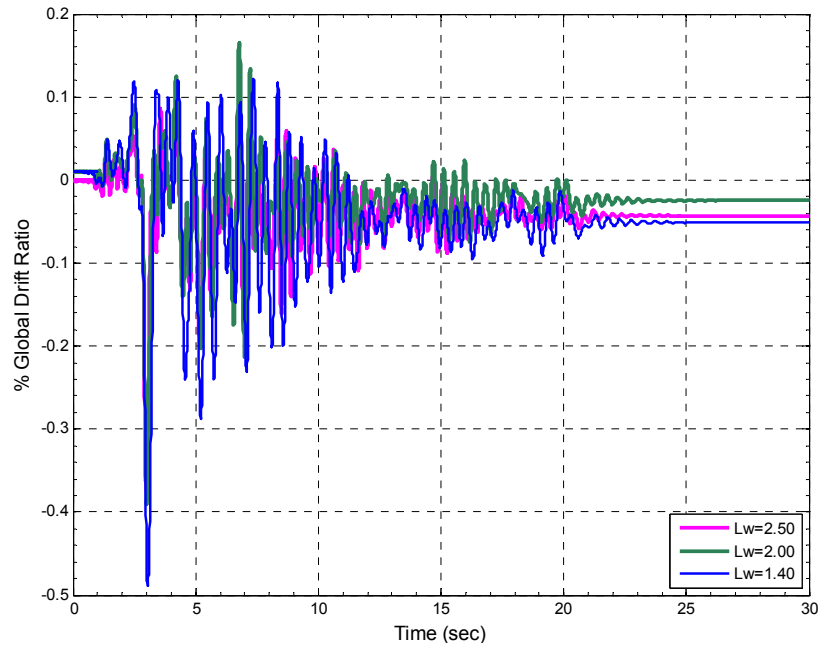


Figure 3.36 – Global Drift Ratio vs. Time History for Erzincan Earthquake Record

It is important to emphasize that the current analyses are only performed under linear geometry; thus the real conditions would exacerbate the responses as presented for the static pushover analysis in subsection 3.2.2.2.

3.3.3 Comparison of Inter-Story Drift Ratios from Static Pushover and Nonlinear Dynamic Analyses

The static pushover analysis performed in Section 3.2 displaces a structure similar to its first mode of vibration, where the first mode in a dynamic analysis basically contributes the most to the response of a structure. Thus, the profiles of inter-storey drifts from dynamic and pushover analyses should be comparable with each other.

For validation of the results between the analyses, the frame without wall system under linear geometry is selected. The maximum global drift ratio of the frame without wall under Erzincan Earthquake in Figure 3.30 is equal to 1%, and the profile of the inter-storey drifts at this instant is plotted in Figure 3.37. The same value for Coalinga Earthquake in Figure 3.29 is 0.3%, and the profile of the inter-storey drifts at this instant is plotted in Figure 3.38. Then, the profiles of inter-storey drifts corresponding to 1% and 0.3% global drifts from the pushover analysis of the frame without wall system under linear geometry and $0.1N_0$ axial load are plotted in Figures 3.37 and 3.38, as well.

The results obtained from pushover and dynamic analyses are observed to be compatible with each other in Figures 3.37 and 3.38.

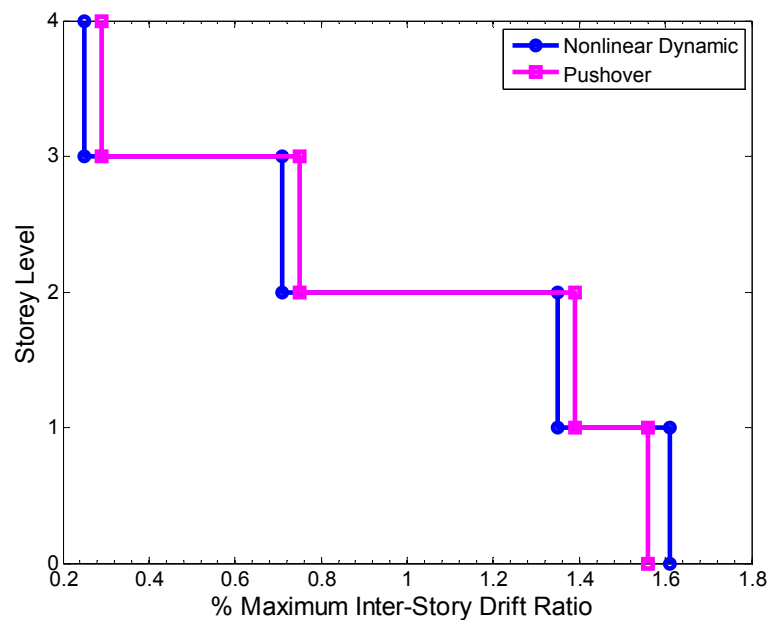


Figure 3.37 – Comparison of the Inter-storey Drifts from Erzincan Earthquake Results and the Pushover Analysis Results of the Frame without Wall System

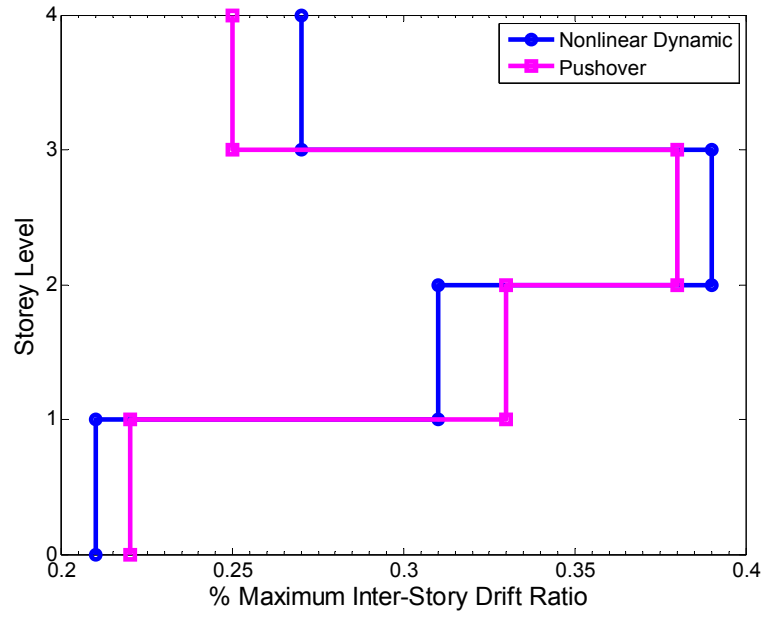


Figure 3.38 – Comparison of the Inter-storey Drifts from Coalinga Earthquake Results and the Pushover Analysis Results of the Frame without Wall System

CHAPTER 4

CONCLUSIONS

4.1 SUMMARY

The objective of this study was to investigate the effect of material and geometric nonlinearities occurring in frame-wall structural systems through the use of advanced frame finite element models and by using static pushover and nonlinear dynamic analysis. Parametric studies on the variation of applied axial force on the structure, change of modeling approaches, and the influence of wall stiffness on the response are investigated. The selected frame systems consisted of beams and columns that are designed according to the strong column and weak beam design approach, thus no soft story mechanism develops.

This thesis consisted of four chapters. The first chapter presented the general information on frame-wall structures and summarized the previous research work done on beam, column and wall finite element models, and the work done on the response behavior of the frame-wall structural systems. In the second chapter, the model of a 4-story and 4-bay building structure was presented, which was later used in the static pushover and nonlinear dynamic analyses. The structural members of the frame without wall and frame-wall structure were designed according

to Turkish Standard TS-500 and Turkish Earthquake Code 2007, and these were modeled by nonlinear beam–column elements in 2-d. OpenSees computer program was used in the overall analyses.

The third chapter of this thesis presented pushover analyses with and without nonlinear geometric effects for the frame structure without wall and the frame–wall structure. Furthermore, dynamic analysis was performed for the same systems, and then the results from the analyses were presented with follow up discussions.

4.2 CONCLUSION

The following can be concluded from the results of the research work presented in this thesis:

- With strong column and weak beam design approach, nonlinear geometric effects in a frame structure without walls could be safely ignored under the application of $0.1N_0$ axial load on the columns, where N_0 is the compressive load carrying capacity of a column.
- With strong column and weak beam design approach, post-yield response of a frame without wall system is significantly altered under the application of $0.2N_0$ axial load on the columns, where localization of damage to a single storey eventually leads to unacceptable levels of inter-storey drift, and soft-storey formation is observed. The situation worsens for the case of $0.3N_0$, where the inter-storey drift for the soft-storey increases suddenly over a small increase in global drift, thus resulting in a brittle response.

- Addition of a wall that satisfies even the minimum requirements of Turkish Earthquake Code 2007 enhances the behavior of a structure significantly and the load carrying capacity increases.
- For the minimum wall length suggested in the code, nonlinearity in the geometry does not alter the ductility of the frame-wall system under the application of $0.2N_0$ axial load on the columns, yet the load carrying capacity of the structure can drop under $0.3N_0$.
- Nonlinearities occurring in the wall could result in significant load redistribution in the rest of the structural members. The columns of a frame-wall structure should be strong enough to resist the forces distributed from the yielding wall, where this incident occurs approximately around 0.25% global drift ratio of the structure for the types of low-rise buildings considered in this thesis.
- The time history analysis provides a scenario to evaluate the response of a structural building, yet the worst case scenario might not have been recorded as an earthquake data. In addition, the response measures obtained from the simulation of a structure under a real earthquake data may not provide a thorough understanding of the strength and ductility of a structure. The use of a static pushover analysis on the other hand provides a practical way of estimating the main characteristics of the load-displacement response under various conditions of loading. Thus the analysis and design of buildings by the code should focus on pushover methods with specific requirements on the obtained load-displacement curves of a building.

4.3 RECOMMENDATIONS FOR FUTURE RESEARCH

The present research focuses on the low-rise RC buildings with and without the presence of structural walls. The following considerations are recommended for future research:

- Mid-rise and high-rise RC buildings with and without the presence of structural walls should be studied through the static pushover analysis.
- The effect of shear failure in the walls could be studied with respect to its influence on the frame-wall.

REFERENCE

Akiş, T., *Lateral Load Analysis of Shear Wall–Frame Structures Ph.D. Dissertation*. 2006, Middle East Technical University, Ankara.

Clark, W.J., *Analysis of Reinforced Concrete Shear Wall-Frame Structures, Ph.D. Dissertation*. 1968, University of Alberta, Canada.

de Souza, R.M., *Force-based Finite Element for Large Displacement Inelastic Analysis of Frames*. 2000, University of California, Berkeley.

Filippou, F.C., *Effects of Bond Deterioration on Seismic Response of R/C Frames*, in *Department of Civil Engineering*. 1983, University of California, Berkeley.

Fintel, M., *Performance of buildings with shear walls in earthquakes in last 30 years*. 1995, PCI Journal. **40**: p. 62-80, Illinois.

Ghobarah, A., and M. Youssef, *Modeling of Reinforced Concrete Structural Walls*. 1999, Engineering Structure. **21**: p. 912-923.

Giberson, M.F., *The Response of Nonlinear Multistory Structures Subjected to Earthquake Excitation*, in *Department of Civil Engineering*. 1967, California Institute of Technology, Pasadena.

Gordon B. Oakeshott, M. G. Bonilla, Don Tocher, William K. Cloud, C. A. Whitten, Karl V. Steinbrugge, Vincent R. Bush, Edwin G. Zacher, Manley W. Sahlberg, D. E. Hudson, and G. W. Housner (1960). "*San Francisco earthquakes of March, 1957*", Bulletin of the Seismological Society of America. **50**: p. 480

Karsan, I.D. and J.O. Jirsa, *Behavior of Concrete Under Compressive Loadings*. Journal of the Structural Division, ASCE, 1969. **95**(ST12): p. 2543-2563.

Katsuhiko, E., and Sehnobrich, W. C., *Inelastic Behaviour of Concrete Frame-Wall Structure*, Journal of the Structural Division, ASCE, 1981. **112**(ST1).

Kayal, S., *Nonlinear Interaction of RC Frame-Wall Structures*, Journal of the Structural Division, ASCE, 1986. **112**: p. 1021-1035.

Kent, D.C. and R. Park, *Flexural Members With Confined Concrete*. Journal of the Structural Division, ASCE, 1971. **97**(ST7): p. 1969-1990.

Kongoli, X., T. Minami and Y. Sakai (1999), "*Effects of Structural Walls on the Elastic-Plastic Earthquake Responses of Frame-Wall Buildings*" Earthquake Engineering and Structural Dynamics. **28**: p. 479-500.

Kotronis, P. and J. Mazars, *Simplified modelling strategies to simulate the dynamic behaviour of R/C walls*. Journal of Earthquake Engineering, 2005. **9**(2): p. 285-306.

McKenna, F., G.L. Fenves, and F.C. Filippou, *OpenSees, Open System for Earthquake Engineering Simulation*. 1999: Berkeley.

Menegotto, M. and P.E. Pinto. *Method of Analysis for Cyclically Loaded Reinforced Concrete Plane Frames Including Changes in Geometry and Non-Elastic Behavior of Elements under Combined Normal Force and Bending*. In *IABSE Symposium on Resistance and Ultimate Deformability of Structures Acted on by Well Defined Repeated Loads*. 1973. Lisbon.

Murty, C.V.R., *Why are buildings with shear walls preferred in seismic region*. 2005, Learning Earthquake Engineering and Construction, India.

Orakcal, K. and J.W. Wallace. *Modeling of Slender Reinforced Concrete Walls*. in *13th World Conference on Earthquake Engineering*. 2004, Vancouver.

Paolo Martinelli, Filip C. Filippou, Maria Gabriella Mulas, *Numerical Simulation of Shaking Table Tests on Reinforced Concrete Shear Wall*. 2007, Studies And Researches **27**.

Paulay, T., M.J.N. Priestley, *Seismic design of reinforced concrete and masonry buildings*. 1992, Wiley, New York.

Saritas, A., *Mixed Formulation Frame Element for Shear Critical Steel and Reinforced Concrete Members, Ph.D. Dissertation*. 2006, University of California, Berkeley.

Spacone, E., F.C. Filippou, and F.F. Taucer, *Fibre beam-column model for non-linear analysis of R/C frames: Part I. Formulation*. *Earthquake Engineering & Structural Dynamics*, 1996. **25**(7 Jul): p. 711-725.

Takayanagi, T., and W. C. Schnobrich, *Computed behavior of reinforced concrete coupled shear walls*, Structural Research Series, vol. 434, University of Illinois, Urbana, 1976.

Taylor, R.L., F.C. Filippou, A. Saritas, and F. Auricchio, *Mixed finite element method for beam and frame problems*. Computational Mechanics, 2003. **31**(1-2): p. 192-203.

Turkish Earthquake Code, *Specification for Structures to be built in Disaster Areas*, Ministry of Public Works and Settlement Government of Republic of Turkey, 2007.

TS-500, *Building Code for Reinforced Concrete*, Turkish Standard, February, 2000

Vulcano, A. and V.V. Bertero, *Analytical Models for Predicting The Lateral Response of R.C. Shear Walls: Evaluation of Their Reliability*, in *UCB/EERC-87/19*. 1987.